Differential Regulation of Opioid Receptors During Inflammation

A THESIS

SUBMITTED TO THE FACULTY OF THE GRADUATE SCHOOL

OF THE UNIVERSITY OF MINNESOTA

BY

Catherine Suzanne Satterfield

IN PARTIAL FULFILLMENT OF THE REQUIREMENTS

FOR THE DEGREE OF

DOCTOR OF PHILOSOPHY

Dr. Christopher N. Honda, Advisor

July 2009

Acknowledgements

I would like to thank the following individuals for their contribution to this thesis work:

Dr. Christopher N. Honda

Cicely Schramm

Erin Nelson

Laura Sorcic

Kanchana Herath

Steph Hacker

Dr. Alvin Beitz

Dr. Donald Simone

Dr. Paul Letourneau

Dr. Heather Wenk

Catherine Harding-Rose

Steve Davidson

Dedication

This dissertation is dedicated to my family and friends.

Abstract

Properties of the opium poppy have been exploited for centuries for the alleviation of pain and to induce euphoria. Classically thought to produce its effects solely in the central nervous system, peripheral opioid analgesic systems are now widely accepted. The activation of these systems leads to a reduction in primary afferent fiber excitability leading to the inhibition of sensory transduction. Opioid receptors function is modulated by a variety of mechanisms. An example of this is enhanced peripheral opioid receptor function following inflammation. The present study examined peripheral opioid receptor regulation in early and late stages of CFA inflammation. Additionally, a new model of UVB of inflammation was characterized. Peripheral MOR receptors are differentially regulated in late and early CFA inflammation. Peripheral MOR is not responsible for attenuated responses of nociceptors to mechanical stimuli 18 hours after CFA inflammation. DAMGO reduced mechanical responsiveness of nociceptors at 72 hours after CFA inflammation in a concentration and antagonist reversible manner indicating that MOR efficacy is enhanced during later stages of CFA inflammation. UVB produced severe but localized inflammation that differed from inflammation produced by CFA. This inflammation sensitizes nociceptor units innervating irradiated skin and results in enhanced peripheral opioid receptor efficacy.

Table of Contents

List of Tables

List of Figures

Chapter 1

Introduction

The analgesic and euphoric properties of the opium poppy have been known for centuries and many cultures have cultivated the plant in order to extract and use the resin for pain relief. Opiates were classically thought to act within the central nervous system and specific binding sites in the brain were first proposed in the 1950s (Beckett and Casy, 1954) and 1960s (Portoghese, 1965). Reynolds (1969) induced profound analgesia by electrically stimulating the midbrain central grey. This finding provided an impetus for the search for the analgesic receptor within the brain. The first solid evidence that opiate's effects were mediated centrally came about in 1973 when three groups almost simultaneously identified opioid receptors in brain tissue (Pert and Snyder, 1973; Simon et al., 1973; Terenius, 1973). This led to the proposal that exogenously applied opiates produced their effects by mimicking endogenous substances that would normally bind to these receptors in the brain. The identification of the endogenous opioid peptides enkephalin (Hughes et al., 1975), beta-endorphin (Li and Chung, 1976) and dynorphin (Goldstein et al., 1979) soon confirmed this.

Peripheral Analgesic Systems

Until recently, opioid induced analgesia was thought to result solely from centrally mediated events. The past decade has gradually led to the understanding that peripheral analgesic systems exist and contribute to the modulation of pain transmission (reviewed in Smith, H., 2008). Opioid

receptors and their endogenous ligands are located at many crucial sites along nociceptive pathways. The activation of these receptors, either by endogenous ligands or exogenous ligands, is thought to modulate pain transduction and sensation. The peripheral branch of the opioid system could be the best target for novel analgesic drugs because it avoids the side effects that centrally administered opioids produce (i.e. tolerance, dependence, sedation, constipation, etc.) and the delivery of drugs peripherally is potentially more direct and uncomplicated. However the peripheral opioid system is incompletely characterized and the efficacy of treatment at the periphery is poorly understood.

To achieve effective peripheral endogenous analgesia, a system must have adequate numbers of functional receptors resulting in decreased pain transmission in addition to sufficient amounts of ligand available to bind to these receptors. Two major peripheral endogenous analgesic systems, cannabinoid and opioid, are reviewed below. Both of these systems satisfy the criteria of having functional peripheral receptors available as well as a localized endogenous source of ligand

Peripheral Cannabinoid System

The activation of cannabinoid receptors, by endogenous or exogenous compounds, represents one major peripheral analgesic system. Cannabinoids have various effects in the body including antinociceptive effects through spinal, supraspinal and peripheral mechanisms (reviewed in

Guindon and Hohmann 2008). Cannabinoids act through the activation of the receptor subtypes CB1 and CB2. CB1 receptors are highly expressed in the central nervous system (CNS) whereas CB2 receptors are mainly found in the periphery including hematopoietic cells and keratinocytes (Munro et al., 1993), peripheral nerve terminals (Griffin et al., 1997) and cultured dorsal root ganglion cells (Ross et al., 2001). Centrally, CB2 has mainly been detected on microglia (Betramo et al., 2006).

Cannabinoid receptors are part a superfamily of G-protein coupled receptors (GPCRs). Activation of CB2 leads to the activation of multiple intracellular signaling pathways resulting in Gi/o-dependent inhibition of adenylyl cyclase and the activation of mitogen-activated protein kinase.

The therapeutic potential of CB2 agonists is being increasingly examined. Activation of peripheral CB2 receptors lead to attenuated inflammatory and neuropathic pain in the periphery without unwanted CNS effects (Malan et al., 2001). The CB2 selective agonist AM1241 suppresses discharge of wide dynamic range neurons through modulation of C-fiber activity and windup most predominantly in the presence of inflammation (Nackley et al., 2004) Recently, peripherally administration on the non-selective cannabinoid receptor agonist WIN 55, 212-2 was shown to attenuate hyperalgesia in a model of cancer pain (Potenzieri et al., 2008).

The interaction of the peripheral nervous system and the cutaneous system may constitute a major endogenous analgesic pathway. Keratinocytes express both CB2 receptors (Casanova et al., 2003) and opioid

peptides (Cabot et al., 1997; Rittner et al., 2001; Kauser et al., 2003). CB2 activation results in indirect analgesia through the release of peripheral beta-endorphin from keratinocytes in epidermis inducing antinociceptive effects through the activation mu opioid receptors on a subset of primary afferent fibers (Ibrahim et al., 2005).

The CB2 receptor is also present on immune cells and activation modulates many neuro-immune interactions including gene expression regulation, chemotaxis, and lymphocyte cell biasing (Cabral and Staab, 2005; Massi et al., 2006).

Peripheral Opioid System

The first serious challenge to the belief that opioids act solely within the CNS came in the late 1970s. Ferreira and Nakamura (1979a; 1979b; 1979c) demonstrated that the intraplantar injection of opiates into inflamed hind paws resulted in peripherally mediated antinociception through the inhibition of second messenger pathways. The importance of peripherally mediated opioid analgesia became more widely accepted (following a study in 1990) in which the mu opioid selective antagonist DAMGO produced antinociceptive effects in the rat hind paw in low doses thought to only produce local effects. Since then, many laboratories have provided evidence for peripheral opioid analgesic systems. These seminal pharmacological and behavioral studies generated interest in the mechanisms responsible for a functional peripheral opioid system.

Peripheral opioid analgesia is enhanced following inflammation and damage. Many mechanisms may be related to this including increased receptor number, enhanced efficacy of receptor, increased number of peripheral terminals (sprouting), and disruption of the perineurium (increased receptor access). These mechanisms are discussed in detail below.

Opioid receptor proteins and mRNA have been detected both in peripheral fibers and their cell bodies located in dorsal root ganglia (DRG) (Chen et al., 1997, Machelska et al., 2006). Although synthesis occurs within the DRG, receptors are intraaxonally transported (in some cases with their mRNA) to both peripheral terminals, and central terminals (Ninkovic et al., 1882; Bi et al., 2006; Hassan et al, 1993) where they become available for membrane insertion. Opioid receptors and peptides are also expressed in peripheral tissues including keratinocytes and melanocytes (Tominaga et al., 2007; Bigliardi et al., 2000).

During inflammation, circulating leukocytes are the predominant source of peripheral opioid peptides. Leukocytes normally travel along the endothelial wall of blood vessels via interaction of adhesion molecules expressed by leukocytes and vascular endothelial cells. Local inflammatory cells and endothelial cells release chemokines following inflammation forming a gradient that attracts leukocytes through chemotaxis. Chemokines also lead to the upregulation of adhesion molecules (Machelska et al., 2002) resulting in leukocyte transmigration through the blood vessel wall and subsequent recruitment to the inflamed area. Substance P, released during

inflammation, also works to recruit leukocytes to areas of inflammation. The substance P receptor NK1 is expressed by peripheral neurons, endothelial cells and infiltrating leukocytes. The antagonization of peripheral NK1 receptors decreases opioid-containing leukocyte recruitment and reduces stress- induced antinociception (Rittner at al., 2007).

Circulating leukocytes are recruited to areas of inflammation and are then able to release opioid peptides. The endogenous ligands (beta-endorphin, dynorphin, and met-enkephalin) for all three opioid receptors have been detected in immune cells following inflammation and tissue injury (Smith, 2003). Polymorphonuclear cells (PMNs) are the predominant source of leukocyte-derived opioids during early stages of inflammation, with monocytes are the main opioid-containing immune cells during later stages. Inflammation also results in the upregulation of the highly selective mu opioid agonists endomorphin 1 and 2 in circulating leukocytes (Mousa et al., 2002). Immune cells also contain opioid peptide precursors (proopiomelancocortin (POMC), proenkephalin) and the enzymes required for post-translational processing (PC-1/3, PC-2) (Smith, 2003). Release of opioid peptides from leukocytes occurs in a receptor selective and calcium-dependent (Rittner et al., 2006) way involving many mediators including corticotrophin-releasing factor (CRF), IL-1 (Schäfer et al., 1994; Cabot et al., 1997, 2001; Binder et al., 2004), and chemokines (Rittner et al., 2006).

Opioid Receptors

Opioid receptors belong to a superfamily of G-protein coupled receptors (GPCRs). All GPCRs consist of seven transmembrane domains linked by alternating intracellular loops (involved with the interaction of G proteins) and extracellular loops (responsible for ligand recognition and binding). There are three major classes of opioid receptors, μ, δ, and κ, (MOR, DOR, and KOR respectively). The binding of ligand induces a conformation change leading to the coupling and activation of one or more G proteins and the initiation of several downstream signaling pathways. Opioids, like most analgesia producing GPCRs, are coupled to Gi/o proteins. Postsynaptically, MOR and DOR agonists induce membrane hyperpolarization through the activation of an inwardly rectifying K+ channel. Presynaptically, agonists prevent neurotransmitter release by inhibiting the opening of high voltage sensitive Ca^{2+} channels, inhibition of tetrodotoxin-resistant sodium channels, and decreased levels of neuronal cAMP. These events typically lead to the receptor-mediated inhibition observed with opioids.

Radioactive binding studies first established the presence of opioid receptors in the spinal cord (Lamotte et al., 1976; Besse et al., 1990). Molecular cloning led to the clear identification of three distinct opioid receptor subtypes, mu opioid receptor (MOR), kappa opioid receptor (KOR), and delta opioid receptor (DOR) (reviewed in Massotte and Kieffer, 1998; Ossipov et al., 2004).

Immunoreactivity has revealed that both MOR and DOR are highly concentrated in the superficial layers of the spinal cord (Dado et al., 1993; Honda and Arvidsson, 1995) where nociceptive C and Aδ sensory fibers principally terminate. In the spinal cord, the majority of DOR and to a lesser extent MOR, are present on central terminals of primary afferent fibers terminating in the spinal cord with the remaining expressed in interneurons and second-order neurons (Besse et al., 1990). All three opioid receptors have been detected in small diameter sensory neurons and their processes (Dado, et al., 1993; Arvidsson et al., 1995; Ji et al., 199; Young et al., 1980; Stein et al., 1990).

Patch-clamp recordings have demonstrated that the inhibitory effects of opiates on isolated rat trigeminal ganglion neurons is through the inhibition of Ca^{2+} channels on small-diameter neurons but not large–diameter neurons through the activation of opioid receptors (Taddese et al., 1995). Similar results have been described for cultured dorsal root ganglion cells from mice (Werz and Macdonald, 1982) and rats (Acosta and Lopez, 1999). Until recently, few studies provided direct electrophysiological evidence for peripheral modulation of sensory neurons by opiates. Locally administered opiates attenuate spontaneous activity in afferent fibers innervating inflamed knee joints of cats (Russell et al., 1987) and in rat polymodal nociceptors irradiated with ultraviolet light (Andreev et al., 1994). Using an *in vivo* skin-nerve preparation, our lab has recently shown that opioid agonists directly applied to the receptive field reduce the excitability of C-fiber nociceptors

innervating inflamed skin, but not normal skin (Wenk et al., 2006; Brederson and Honda, personal communication).

Inflammation and Modulation of Peripheral Opioid Receptors

Damage sensing nociceptive neurons detect injury and noxious stimuli and respond by triggering local release of pro-inflammatory neuropeptides and cytokines that leads to the recruitment of immune cells and sensitization of primary afferent fibers (Willis, 1999). The cutaneous system also contributes to the detection of injury and noxious stimuli through the further release of pro-inflammatory cytokines and peptides. The resulting inflammation leads to further production and release of numerous inflammatory mediators that can stimulate and/or propagate pain (reviewed in Julius and Basbaum, 2001). Related to this, inflammation and tissue injury also lead to increased opioid receptor synthesis, transport, accessibility, and efficacy. The analgesic effects of peripherally applied opiates are much more pronounced following inflammation while little effect has been demonstrated in normal tissue.

Using the CFA model of persistent pain, researchers have shown that local injection of systemically inactive doses of MOR, KOR, and DOR selective agonists dose dependently attenuate nociceptive responses (Stein et al., 1989). Selective antagonists reversed these effects. Analgesic effects of peripherally applied opiates can occur within hours of inflammatory onset (Czlonkowski et al., 1993; Antonijevic et al., 1995; Zhou et al., 1998; Wenk et

al., 2003). Peripherally applied morphine and deltorphin II, a DOR selective agonist, attenuate responses of sensitized C-fiber nociceptors in skin inflamed for 18 hours (Wenk et al., 2006) providing evidence for functional competence of peripheral opioid receptors.

An increased number of receptors can account for some enhancement of receptor function though it is unlikely that increased transcription and transport accounts for early time periods due to the time it takes for the receptor to be transcribed and travel down the axon. Following CFA inflammation, beta-endorphin binding is elevated in sciatic nerves within 24 hours (Hassan et al., 1993) and opioid receptor immunoreactive cell bodies are elevated within 4 days (Stein et al., 1990). Increased access to existing receptors is another mechanism that could account for enhanced receptor function. Inflammation leads to the breakdown of the perineurium sheath improving access of available ligand. Endogenous ligand is increased following inflammation mainly due to opioid-containing leukocytes as well as release by keratinocytes (Ibrahim et al., 2005; Bigliardi et al., 2000). The presence of ligand can mediate translocation of opioid receptors from internal stores to the plasma membrane (Coggeshall et al., 1997).

Modulation of receptor function may account for marked differences following inflammation. As stated previously, the analgesic effects of peripherally administered opiates are enhanced under inflammatory conditions. Opioid agonists can have inhibitory, stimulatory, or no effect on sensory neurons. It is hypothesized that opioid receptors couple to different

downstream signaling pathways depending on cellular conditions (Patwardhan et al., 2005). Differences in downstream signaling by MOR and DOR have also been reported (Reviewed in Law and Low, 1999). Previous studies have also shown that the activation of one G-protein coupled receptor can alter the function of another G-protein coupled receptor. For example, bradykinin, which released from mast cells and blood vessels during injury and inflammation, induces trafficking of DOR to the plasma membrane of trigeminal nociceptors. DOR then gains function competence through activation of bradykinin receptors located on sensory nerve fibers (Patwardhan et al., 2005).

Effects of Ultraviolet Radiation on Inflammation and Opioid Analgesia

The effects on human skin have been well documented and include inflammation, erythema, photo-aging, thermal hyperalgesia and mechanical allodynia (Young et al, 1985; Harrison and Young, 2002). Acute skin over-exposure to ultraviolet (UV) radiation has recently been proposed as an inflammatory pain model in both rats and humans (Hoffmann and Schmelz, 1999; Davies et al., 2005; Bishop et al., 2007).

Broadband acute UV radiation leads to the release of neuropeptides, histamine, prostaglandins, serotonin and free radicals in addition to both pro and anti-inflammatory cytokines (Benrath et al., 1995; Eschenfelder et al., 1995; Saade et al., 2000). These factors most certainly contribute to reported sensitization, though the mechanisms are poorly understood. Early research

used wide band UV light that is mostly comprised of light in the UVA wave range. Recently, a UVB model of inflammatory pain has been proposed (Bishop et al., 2007). This UVB model is ideal for electrophysiological examination of the effects of UV irradiation on sensory fibers because UVB is predominantly absorbed in the epidermis where epidermal sensory fibers terminate. Few electrophysiological studies on the effects of UV irradiation have been performed. In two such studies, UVA irradiation led to the sensitization of primary afferent fibers characterized by increased excitability and spontaneous discharge (Szolcsanyi et al., 1988; Andreev et al., 1994).

Unlike commonly used persistent inflammatory agents like Complete Freund's Adjuvant (CFA) and carraggenan, UV irradiation is not based on the injection of antigen activation of a large scale innate immune response and subsequent activation of acquired immunity. Further characterization of an animal model may provide a useful translational tool for the study of a distinct type of inflammatory pain

Statement of Purpose

There is increasing behavioral, anatomical and electrophysiological evidence for the existence of peripheral opioid receptors on peripheral terminals of primary afferent fibers, as well as non-neuronal cutaneous cells and circulating immune cells. During tissue inflammation, several underlying mechanisms result in increased opioid receptor number and efficacy to produce peripherally mediated analgesia.

The goal of this thesis is to characterize peripheral opioid-mediated analgesia in two models of persistent pain. Specifically, functional changes in the opioid receptor responsible for morphine induced analgesia following CFA inflammation will be examined using electrophysiological techniques. Additionally, a new persistent pain model based on UVB irradiation will be characterized and compared to the commonly used CFA model. Finally, the effects of peripherally applied opiates after inflammation with the UV model will be examined.

In Chapter 2, the functional state of peripheral MOR will be examined during both early and late stages of CFA inflammation. Previous work from our lab has shown that morphine attenuates both thermal and mechanical responses of C-fiber nociceptors 18 hours following CFA inflammation (Wenk et al., 2006). More recent studies, using the DOR selective agonist deltorphin II, demonstrated that DOR is most likely responsible for the effects of morphine on nociceptor excitability during this stage of inflammation.

MOR synthesis and trafficking has been demonstrated during later stages of CFA inflammation and therefore MOR may be involved in peripheral opioid analgesia during later stages of CFA inflammation (Hassan et al., 1993; Machelska et al., 2006). Using the selective MOR agonist, DAMGO, we examined MOR's involvement in peripheral opioid analgesia in both late and early stages of CFA inflammation.

The specific hypothesis examined was that MOR receptors are differentially regulated during early and late stages of CFA inflammation.

To test this hypothesis, an *in vitro* skin-nerve preparation was used to examine the effects of the MOR selective agonist DAMGO on mechanical response properties of identified single units in skin 18 and 72 hours after CFA-induced inflammation. The effects of morphine sulfate on mechanical responses to noxious mechanical stimuli were also examined. Additionally, changes in the type and number of single units sensitive to both morphine and DAMGO at later stages of inflammation were observed as well as receptor efficacy.

Chapter 3 describes a new model of persistent pain and inflammation in the adult rat induced by UVB irradiation. Irradiation of the rat hind paw resulted in pronounced thermal hyperalgesia and mechanical allodynia. Histological examination of skin demonstrated this model induces immune cell infiltration, epidermal separation and necrosis. Using an *in vivo* skin-nerve preparation, single units were recorded from tibial nerve and mechanical and thermal properties were characterized.

The specific hypothesis that these experiments sought to test was that UVB irradiation leads to sensitization of primary afferent fibers. In addition, UVB results in pronounced inflammation that differs from inflammation induced by CFA.

To test this hypothesis, the classical signs of inflammation were measured, hyperalgesia, heat, and swelling. Redness was also recorded. Histological characterization was used to examine immune cell infiltration as well as edema, cell death, and the general type of immune response mounted. Single primary afferent fibers from irradiated skin were electrophysiologically characterized and compared to normal skin. Responses to both mechanical and thermal stimuli were examined.

In Chapter 4, the model described in Chapter 3 was utilized to examine the responses of identified single units to morphine under normal and inflammatory conditions.

The specific hypothesis this study examined was whether UVB leads to sensitization of identified nociceptors and like the previously studied CFA model of inflammation whether this sensitization leads to the activation of endogenous peripheral analgesic systems. We further hypothesized that mechanical sensitization would be attenuated by morphine sulfate.

The *in vivo* skin-nerve preparation will be used to examine morphine's effect on identified single units in skin 48 hours after UVB irradiation. This time point was chosen because it corresponds to the time where behavioral sensitivity is seen following irradiation as well as histopathological evidence of severe inflammation and immune responses.

CFA is a common animal model used to study mechanisms underlying pain. There are however problems with this model. This model produces an

intense immune response due to the injection of foreign material. The immune response is characterized by a large influx of PMN cells that searches out and destroys foreign material. Unfortunately, the immune response is very broad and is not due to any specific receptor-mediated event so it is difficult to ascertain the cause source of CFA-induced effects.

Further characterization of the UVB model can lead to a new translational model of inflammatory pain. The immune system can mount several types of responses and in each to varying degrees. More inflammatory animal models will allow for a greater understanding of inflammatory conditions and could lead to more specific analgesic targeting. The UVB model offers a number of advantages to the CFA model. First, it is considered a sterile model. Changes in tissue are considered to be due to changes within the tissue instead of resulting from a response to foreign material. Secondly, UVB rays terminate mainly in the epidermis localizing the origin of inflammation. Thirdly, CFA-induced inflammation cannot be used in human research. UVB irradiation has been shown to cause reliable sensitization in humans (Koppert et al., 2004). Additionally, UVB irradiation models the common human ailment of sunburn. Until recently, most evidence for this was psychophysical reports in humans but recent electrophysiological studies provide direct evidence of nociceptor sensitization (Szolcsanyi, 1987; Andreev et al., 1994). Lastly, problems were encountered during our electrophysiological recordings in skin at later stages of CFA-induced inflammation. Nerve fibers were more likely to break during teasing possibly

due to changes in the perineurium. The extreme degree of inflammation produced by CFA was most likely responsible for these effects.

A further understanding of peripheral analgesic systems could potentially lead to therapies that are able to mimic or augment these systems and produce analgesia in the absence of centrally produced side-effects (respiratory depression, addiction, tolerance, constipation and drowsiness). Localized targeting of peripheral receptors could greatly reduce these detrimental side effects and in turn enhance the clinical effectiveness of opioid therapies.

Chapter 2

Function of Peripheral Mu-Opioid Receptors is Differentially Regulated During Early and Late Stages of Inflammation

Introduction

Morphine was once thought to exert its effects solely through its action on opioid receptors in the central nervous system. It is now understood that opioid receptors are present in peripheral tissues as well as on peripheral processes and terminals of sensory fibers (Coggeshall et al., 1997; Stander et al., 2002, Wenk and Honda, 1999). Peripheral opioid receptors are present in healthy tissue, but peripherally applied opiates have little effect on nociceptive excitability. Furthermore, the actions of peripheral opioid receptors are enhanced under inflammatory conditions. Consistent with this, peripherally applied opiates have anti-hyperalgesic effects in both animal behavioral models and in human clinical trials when applied to inflamed tissues (Joris et al., 1987; Stein and Yassouridis, 1997).

Until recently, little direct evidence for functional peripheral opioid receptors existed. Patch-clamp recordings have demonstrated the inhibitory effects of opiates on isolated sensory cells through the inhibition of Ca^{2+} channels (Taddese et al., 1995, Werz and Macdonald, 1982, Acosta and Lopez, 1999). Peripherally administered opiates attenuate spontaneous activity in afferent fibers innervating inflamed knee joints of cats (Russell et al., 1987) and in ultraviolet irradiated cutaneous polymodal nociceptors in rats (Andreev et al., 1994).

Previously, we provided electrophysiological evidence for functional opioid receptors on peripheral terminals of primary afferent fibers in skin 18

hours following CFA inflammation. Using an *in vitro* glabrous skin-nerve preparation, the effects of morphine on mechanical and thermal response properties were evaluated in nociceptors innervating normal of inflamed skin. Morphine had no significant effect on nociceptor responses to noxious mechanical and thermal stimuli, but reduced responses to both mechanical and thermal stimuli in 58% of nociceptors innervating inflamed skin (Wenk et al., 2006). These electrophysiological findings support that inflammation leads to increased efficacy of peripheral opioid receptors.

It is unclear what opioid receptors are responsible for morphine's effects on peripheral nociceptors innervating inflamed skin. All three opioid receptors have been detected in small diameter sensory neurons and on their peripheral processes (Dado, et al., 1993; Arvidsson et al., 1995; Ji et al., 199; Young et al., 1980; Stein et al., 1990). Following CFA induced inflammation, beta-endorphin binding is elevated in sciatic nerves within 24 hours (Hassan et al., 1993) and opioid receptor immunoreactive DRG is elevated 4 days after CFA injection (Stein et al., 1990).

To determine which opioid receptors are responsible for the inhibition of mechanical responses by morphine, we evaluated the effect of the DOR selective agonist deltorphin II on the mechanical response of nociceptive units innervating skin 18 hours CFA inflammation. Deltorphin II inhibited the mechanical responses of a subset of nociceptive units innervating inflamed skin in a concentration dependent antagonist reversible manner but had no effect on normal healthy skin. This provided the first electrophysiological

evidence for the existence of functional peripheral DOR in inflamed skin (Brederson and Honda, personal communication).

The present study examined the role of MOR on the effect of morphine has on the mechanical response of nociceptors innervating skin 18 hours following CFA inflammation. Using the *in vivo* glabrous skin-nerve preparation, the effect of the MOR selective agonist DAMGO on mechanical responses of identified nociceptors was evaluated.

It is also clear that inflammation leads to modulation of opioid receptors. Following inflammation, MOR synthesis is increased in peripheral cell bodies and axonal transport is enhanced leading to increased receptor availability (Stein et al.1997, Hassan et al., 1993; Mousa et al., 2001). In addition, inflammatory conditions may lead to increased receptor efficacy. To address whether MOR is regulated during early and late stages of inflammation, the present study also examined the effects of morphine sulphate and DAMGO on the mechanical responses of identified nociceptors innervating skin 72 following CFA inflammation.

Methods

Animals

All experimental procedures were approved by the Institutional Animal Care and Use Committee at the University of Minnesota and conform to

established guidelines. A total 67 adult male Sprague-Dawley rats, 250-350 g were used in this study.

Induction of Inflammation

Adult male Sprague-Dawley rats (250-400 grams; *n*=92) were used in all experiments according to the Institutional Animal Care and Use Committee at the University of Minnesota. Rats in the inflamed group were deeply anesthetized with isoflourane and received a unilateral subcutaneous injection of CFA (100 μl, emulsified 1:1 with saline) into the plantar surface of the hindpaw, eighteen and 72 hours prior to experimentation.

Glabrous Skin-nerve Preparation

Rats were deeply anesthetized with a combination of ketamine, acepromazine and xylazine (6.8/0.09/0.45 mg/kg). The glabrous skin of the hindpaw was dissected and excised together with the attached tibial nerve and the medial and lateral branches of the plantar nerve. The skin-nerve preparation was immediately transferred to a chamber that was continuously perfused (≥ 18 ml per minute) with warmed to (30±2°C), oxygen-saturated synthetic interstitial fluid [SIF; containing in mM) 123 NaCl; 3.5 KCl, 0.7 $MgSO_4$, 2.0 $CaCl_2$, 9.5 Na gluconate, 1.7 NaH_2PO_4, 5.5 glucose, 7.5 sucrose, 10.0 Hepes; pH 7.45±0.05, 290±0.05 mOsm] (Koltzenburg et al. 1997). The preparation was placed corium side up and anchored with insect pins. The preparation was further dissected until the skin and nerve were cleared of all

tendons, muscles, and vasculature. The cut end of the tibial nerve was threaded through a small aperture into a recording chamber and placed on top of a mirrored dissection platform. The recording chamber was filled with buffer below and oil above the mirror.

Electrophysiological Procedures

Compound Action Potential

A compound action potential was recorded at the beginning of most experiments (Figure 1). An insulated monopolar stimulation electrode was placed on the main trunk of the medial or lateral plantar nerve. The tibial nerve was lifted onto a fine gold electrode with fine forceps for extracellular recording. The recording electrode was suspended in oil and referenced to the bath. Stimulating current was delivered with increasing intensity until each waveform component of the compound action potential ($A\alpha\beta$, $A\delta$, and C) could be evoked. The rate of conduction measured for each waveform was expressed as meters per second. Electrical signals were amplified differentially (DAM80, World Precision Instruments, Austin, TX), filtered, then routed in parallel to an oscilloscope and computerized data acquisition system.

Isolation and Characterization of Single Units

Two search strategies were used to characterize single units. First, small bundles of nerve fibers were placed on the recording electrode, and a hand-held glass rod was used to gently probe for area of innervation on the corium surface of the skin. Second, an electrical search stimulus was used to isolate single fibers. Filaments were progressively divided and placed on the recording electrode until single unit activity could be isolated. A roving stimulating electrode was traced along the plantar nerve branches until the receptive field could be electrically identified. The stimulating electrode was positioned in the cutaneous receptive field and an electrically evoked spike was recorded to determine the latency from the stimulus to the spike. Distance was measured using thin suture placed along nerve. Conduction velocity was expressed as meters per second.

Spontaneous Activity

Unevoked baseline activity was recorded for at least 15 seconds before each mechanical stimulus. Spontaneous activity was defined as firing ≥ 1 spike/sec in the absence of any intentional stimulus.

Mechanical Response Properties

Mechanical response properties were determined using a combination of two methods. First, mechanical threshold was determined using calibrated von Frey filaments applied to the corium surface in order of increasing

pressure. Filaments ranged from 0.5 mN to 96.5 mN. Mechanical threshold was defined as the lowest force to evoke an action potential response 50% of the time. Stimulus-response relationships were then determined for each unit. Responses were measured using constant pressure of 0.5, 1.8 and 3.3 bars delivered with weighted probes having a diameter of 2.5 mm. Later experiments used a computer controlled mechanical probe (Aurora Scientific Inc. Ontario, Canada) which a diameter of 1.2mm that produced a graded pressure (0.5–4.0 bars). Nociceptors were defined as units whose firing rate increased monotonically with increasing pressure of stimulation. High threshold units that responded only to the maximal stimulus were also defined as nociceptors. Each probe was positioned in a micromanipulator and lowered onto the receptive field for a five second stimulation. The stimulation onset and offset times were signaled to the online data acquisition program.

Repeated Mechanical Stimulation of the Receptive Fields

Units were tested for reproducibility and variability of their responses to multiple mechanical stimulation trials. Baseline responses to suprathreshold mechanical stimulation of the corium receptive fields of single units were assessed using a computer controlled mechanical probe. Two to three mechanical stimulations of were recorded before drug testing to measure baseline (BL) responses (in spikes). The mechanical stimulation was delivered every 2 minutes each with duration of 5 seconds.

Peripheral Drug Testing

Preparation of Drugs

Synthetic interstitial fluid solution (SIF; on mM: 123 NaCl; 3.5 KCL, 0.7 MgSO4, 2.0 CaCl2, 9.5 Na gluconate, 1.7 NaH2PO4, 5.5 glucose, 7.5 sucrose, 10 HEPES; pH 7.45 ± 0.05) (Koltzenburg et al., 1997) was prepared no more than one day prior to each experiment and stored at 4°C. Stock solution of morphine sulfate, DAMGO and naloxone (Sigma; St. Louis, MO) were diluted with SIF (ph 7.45 ± 0.05).

Stock solutions of morphine sulfate (1mM), naloxone (100μM), and DAMGO (100μM); (Sigma-Aldrich, St. Louis, MO) were made in water and stored at 4°C. Working concentrations of the ligand were diluted in SIF, as needed. Each drug solution and vehicle was warmed to room temperature and saturated with oxygen prior to use. Both SIF and drug solutions were oxygen-saturated before use.

Drug Application and Receptive Field Stimulation

Using a glasses probe the receptive field of mechanically sensitive units was determined. A small plastic cylinder (8mm or 12mm) was sealed over the receptive field with petroleum jelly or vacuum grease, filled with SIF, and served as a reservoir for drug delivery. SIF was then replaced with solutions of morphine sulfate, DAMGO, DAMGO plus naloxone, morphine sulfate plus naloxone, naloxone only, or vehicle and applied for two minutes.

The receptive field was mechanically stimulated every two minutes using a dual-mode lever system. Recovery was defined as a return to baseline firing rate by about at least 50% after drug application. Units that did not recover were excluded from this study. Data are reported as the mean percent of baseline firing± standard error (sem) for each unit unless otherwise noted.

Data Collection and Analysis

Compound action potential and teased fiber recordings were collected using a data acquisition program written on the LabView platform (LabView 5.1; National Instruments) or Spike 2 software (CED; Cambridge, UK). Data were analyzed on- and off-line. Offline data analysis was conducted with an in-house spike discrimination program designed for LabView 5.1 or using Spike 2. Values are expressed as mean ± sem unless otherwise noted.

Results

Compound Action Potentials and Classification of Single Units by Conduction Velocity

Compound actions potentials were recorded from tibial nerve at the beginning of most experiments to be used to classify single units by conduction velocity. A small percentage of compound action potentials were recorded from either the medial or lateral plantar nerve. No significant

difference was observed between compound action potentials recorded in skin inflamed for 18 hours compared to skin inflamed for 72 hours, so for the purpose of the study the values were combined.

The conduction velocity ranges of all three major wave components (Aβ, Aδ and C) are expressed as mean ± standard error (sem) and summarized in Table 1. The average mean conduction velocity for the Aαβ wave component was 29.2 ± 7.0 m/s with an average maximum and minimum conduction velocities of 50.3 ± 15.0 m/s and 17.1 ± 4.2 m/s respectively. The Aδ wave had a mean conduction velocity of 10.3 ± 2.9 m/s and ranged from 16.1 ± 3.3 m/s and 5.6 ± 2.6 m/s. The C wave had a mean conduction velocity of 0.82 ± 0.2 m/s and ranged from 1.10 ± 0.2 m/s and 0.70 ± 0.1 m/s.

The Aδ and C wave components did not overlap. The minimum conduction velocity for the Aδ wave was 2.7 m/s while the fastest C conduction velocity recorded was 1.7 m/s. Based on the above measurements, single units were classified as follows. Units with conduction velocities greater than 17 m/s were considered to conduct in the Aβ range. Those conducting between 17 m/s and 3 m/s were classified as Aδ units. Units conducting below 1.7 m/s were considered C fibers. Units that had conduction velocities that fell between the Aδ and C wave components of the compound action potentials (conducting between 3 and 1.7 m/s) were assigned to a C/Aδ classification.

Classification of Single Units

Single Units Innervating in 18 hour Inflamed Skin

Thirty-two units isolated from tibial nerves of 19 rats were included in this study (Table 1). All units were isolated from skin 18 hours after CFA inflammation. Eighteen of these units conducted within the C fiber range with a mean conduction velocity of 0.91 ± 0.23 m/s. Nine units conducted within the C/Aδ range with a mean conduction velocity of 2.27 ± 0.34 m/s and five units conducted within the Aδ range with a mean conduction velocity of 7.60 ± 2.67 m/s.

All single units studied were identified as nociceptors because they fit the criteria that their firing rate increased monotonically with increasing pressure of stimulation.

All three fibers classifications examined showed reduced median mechanical thresholds compared to those innervating normal skin (Table 1). Furthermore, Aδ-fibers and C-fibers had reduced thresholds to those innervating skin inflamed for 72 hours. Median mechanical thresholds for those units innervating 18 hour inflamed skin were: Aδ, 37.74 mN; C/Aδ, 10 mN; C, 18.24 mN.

Units with a firing rate ≥ 1 spike/sec in the absence of applied stimulus were classified as spontaneously active. Spontaneous activity was recorded in 10 out of 32 units (31%); 6 of 18 C-fiber units (33%), 2 of 9 (22%) C/Aδ-fiber units, and 2 of 5 (40%) of Aδ-fiber units (Table 1).

Single Units in 72 hour Inflamed Skin

A total of 89 units were recorded from isolated units innervating skin 72 following CFA inflammation (Table 1). Forty-nine units conducted within the C-fiber range with a mean conduction velocity of 0.91 ± 0.27 m/s. Twenty-two units had conduction velocities within the C/Aδ range with a mean conduction velocity of 2.53 ± 0.4 m/s and seventeen units conducted in the Aδ range with a mean conduction velocity of 7.46 ± 2.9 m/s. One unit conducting in the Aβ with a conduction velocity of 18.1 m/s.

All single units studied were identified as nociceptors because they fit the criteria that their firing rate increased monotonically with increasing pressure of stimulation.

All fiber types (Aδ, C/Aδ, C) studied showed reduced mechanical thresholds compared to units innervating normal skin (Table 1). Median mechanical thresholds were as follows: Aδ, 14.55 mN; C/Aδ 10 mN; C, 37.75 mN.

Spontaneous activity was observed in 36 out of 89 units (40%) examined; 19 of 49 C-fiber units (39%), 9 of 22 (41%), C/Aδ-fiber units and 6 of 17 (35%) of Aδ-fiber units (Table 1).

Thirty-eight individual units were recorded from normal healthy skin. Of these, 4 were treated with morphine and 5 were treated with DAMGO (Table 1). Mean conduction velocities did not differ from units innervating inflamed skin (Aδ, 10.3 ± 2.1 m/s; C/Aδ, 2.8 ± 0.48 m/s; C, 1.0 ± 0.43 m/s).

Fewer units were classified as nociceptors though all units tested with drug were nociceptors.

There was a pronounced decrease in the number of fibers with spontaneous activity. Eighteen percent of all fibers tested demonstrated spontaneous activity compared to 40% of units innervating 72 hour inflamed skin and 31% of units innervating 18 hour inflamed skin. Furthermore, units innervating inflamed skin had reduced median mechanical thresholds compared to units innervating normal skin (Aδ, 63.2 mN9; C/Aδ, 18.24 mN, C, 82.5 mN), indicating units innervating inflamed skin were sensitized.

Response Variability and Criteria for Drug Effect

Data values for response variability are expressed as mean ± standard deviation.

A large amount of variability was present in the individual responses of sensitized nociceptors. In order to differentiate a true drug effect from normal variability the reproducibility of single unit responses to repeated mechanical stimulation was assessed for most units using a computer controlled mechanical probe. Responses from units innervating 18 and 72 hour CFA inflamed skin did not differ and data was combined. Two to three mechanical stimulations were recorded before drug testing to measure baseline (BL) responses (in spikes) (Figure 3). The ratio of spikes between BL 1 and BL 2 was measured and the ratio of spikes between BL 2 and BL 3. The average

BL ratio was then measured. The ratio of BL 1 and BL 2 was used as the average if only two BL measurements were obtained. The mean BL spike ratio of all units was 1.00 ± 0.14% confirming that the units used had reproducible responses. Units that had responses within 2 standard deviation s of the mean BL were further examined.

Values that ranged within 2 standard deviations above or below the mean BL response all units were considered within normal variability. Therefore, for a unit to have a positive drug response, the percent of baseline response after drug for each unit was less than 72% or greater than 128% of its baseline response. Percent baseline response for each unit is the ratio of the mean response (in spikes) calculated after drug divided by that units mean baseline response (in spikes).

Effect of Morphine Sulphate on Neuronal Excitability in Skin inflamed for 72 Hours

A total of 51 units from 30 rats were tested with morphine sulphate 72 hours following CFA inflammation. The range of concentrations of morphine tested in inflamed skin included 100 nM (n=4), 300 nM (n=9), 500 nM (n=22), 700 nM (n=9), and 1 μM (n=7). The mean (± sem) percent baseline responses for all units tested with MS are as follows: 100 nM 94.9 ± 14.2%, 300 nM 91.24 ± 8.8%, 500 nM 70.12 ± 7.8%, 700 nM 78.6 ± 8.4%, and 1 μM 68.6 ± 13.7% (Figure 4). As a population, the mean percent baseline responses for fibers treated with the 500 nM, 700 nM and 1 μM ranges were

significantly different than vehicle treated fibers (mean percent baseline response 97.1 ± 3.6%).

Five morphine sensitive units were treated with a co-application of 500 nM morphine sulphate + naloxone after a washout period of at least 30 minutes after first exposure to morphine. Naloxone blocked the effects of morphine of mechanical responses of all units indicating the response is receptor mediated.

All units that met the criteria for a positive drug effect (responder) were grouped together. A total of 16 of 51 (31%) units had decreased mechanical responses following morphine application with a mean percent baseline response of 39.99 ± 4.5% (Figure 5).

Effect of DAMGO on Single Units Innervating 18 Hour Inflamed Skin

A total of 23 units with conduction velocities between 0.11 and 12.40 m/s were tested with DAMGO. Mean population responses before, during, and after drug application were recorded. The range of concentrations tested was 100nM (n=6), 300nM (n=5), 500nM (n=4), and 1 μM (n=8). Following drug application, the mean (± sem) percent baseline responses were as follows: 100 nM 105.0 ± 6.0 %, 300 nM 93.2 ± 5.3%, 500 nM 109.1 ± 4.0% and 1 μM 86.47 ± 9.0% (Figure 6). Ten units were treated with vehicle before treatment with DAMGO or with vehicle only. Vehicle treated fibers had a mean percent baseline response of 97.42 ± 2.5 %. Population data for all

concentrations of DAMGO did not significantly differ from vehicle treated fibers.

A total of 2 of 23 units (9%) met the criteria for a responder to the application of DAMGO meaning the response of each unit decreased by 72% following drug application, followed by a return to 50% of the mean baseline. One of 5 units (20%) had decreased response to mechanical stimulation following application of 300 nM DAMGO. The mean percent baseline response was 70.2 %. One of 8 units (21%) treated with 1 μM DAMGO had decreased response to mechanical stimulation. Both of these responses were inhibited by the opioid antagonist naloxone.

In order to determine whether a basil level of endogenous peripheral opioid inhibition is mediating responses of primary sensory fibers, 1 μM naloxone was applied to the receptive fields of 3 isolated units. The mean percent baseline response of the units to naloxone was 96.84 ± 3.0%. This was not significantly different from vehicle suggesting that endogenous opioid activity is not mediating the responses of these units. Co-application of 1 μM naloxone + 500 nM DAMGO also did not have an effect on mechanical responses of nociceptors. Mean percent baseline response of these fibers was 104.8 ± 7.2% (Figure 6).

Effect of DAMGO on Single Units Innervating 72 Hour Inflamed Skin

In order to determine whether changes in MOR activity or availability occurs between early and late stage of inflammation, the effect of DAMGO on

neuronal excitability was tested in isolated sensory fibers innervating skin inflamed with CFA for 72 hours. During this time, increases in MOR synthesis and trafficking have been documented as well as changes in inflammatory conditions.

A total of 21 units innervating skin 72 hours after CFA inflammation were recorded from 17 rats. The following concentrations of DAMGO were applied to the receptive fields of isolated units: 100 and 300 nM (n=4), 500 nM (n=8); 700 nM (n=6), 1 μM (n=3). The responses of fibers treated with DAMGO were compared to all fibers innervating 72 hour inflamed skin treated with vehicle (mean percent baseline 97.1 ± 3.6%). Mechanical responses of units treated with 500 nM, 700 nM and 1 μM were significantly reduced following DAMGO application with the following mean percent responses, 71.71 ± 9.1%, 72.84 ± 13.0%, and 54.16 ± 26.5% respectively. Three DAMGO sensitive units received a co-application of 500 nM DAMGO + 1 μM naloxone 30 minutes after drug washout. Co-application blocked the effect of DAMGO indicating the effect was receptor mediated.

Criteria for a positive drug effect on single units are described above. Data from units demonstrating a decrease in responsiveness to mechanical stimulation after application of DAMGO followed by a return to 50% of baseline response are shown in figure 8. A total of 10 out of 21 (48%) units met the criteria for a positive drug effect. The following data points were obtained: 300 nM (n=2), 500 nM (n=4), 700 nM (n=2) and 1 μM (n=2).

DAMGO inhibited single-unit responses in a dose-dependent naloxone inhibited (Figure 7) manner.

Effect of Opiates on Mechanical Responses in Inflamed skin and Normal Skin.

We have shown previously that morphine fails to reduce mechanical responses in normal skin (Wenk et al., 2006). Using a protocol that enabled constant recording of mechanical responses every two minutes we tested both 500 nM morphine and 500nM DAMGO on isolated units innervating skin inflamed for 72 hours or normal skin. These doses were selected because it resulted in reduced responses in at least half of all units when tested in inflamed skin. Values are all units tested for each category and are expressed as mean ± sem. Morphine and DAMGO significantly altered mechanical responsiveness in units innervating inflamed skin. Morphine reduced mechanical responses to 70.2 ± 7.8% of baseline and DAMGO reduced responses to 71.7 ± 9.1%. Vehicle did not have an effect on responsiveness regardless of skin condition.

Discussion

The aim of the present study was to investigate whether peripheral MOR alters mechanical responses of cutaneous primary afferent fibers. The MOR-selective agonist MOR was applied to the cutaneous receptive field of isolated Aδ, C/Aδ, and C-fibers innervating skin inflamed for either 18 or 72

hours by subcutaneous injection of CFA. Furthermore, the effect of morphine sulphate was tested on skin inflamed for 72 hours in order to compare to results previously obtained by our lab on C-fibers innervating skin inflamed for 18 hours.

Units innervating both 18 and 72 hour inflamed skin exhibited characteristics of sensitization including reduced mechanical thresholds, increased spontaneous activity, and increased responses to suprathreshold mechanical stimuli. Morphine sulphate reduced mechanical responses of units innervating 72 hour inflamed skin. DAMGO did not have a significant effect on mechanical responses in units innervating inflamed skin but did reduce 48% of all units innervating 72 hour inflamed skin. These findings suggest that changes occur during early and late stages of CFA inflammation to regulate MOR function.

Sensitization of Single Cutaneous Fibers

Previous research from our lab has demonstrated sensitization of C-fibers innervating 18 hour inflamed skin including decreased mechanical thresholds, increased spontaneous activity and elevated responses to suprathreshold mechanical and thermal stimuli (Wenk et al., 2006; Brederson and Honda, in press). Sensitization of primary afferent fibers is associated with decreased response threshold and increased responsiveness to suprathreshold stimuli and increased spontaneous behavior (Raja el al., 1999; Treede et al., 1992). Sensitization to thermal stimuli is well

documented (Campbell and Meyer, 1983; LaMotte et al., 1982) but sensitization to mechanical stimuli is less clear. Findings consistent with sensitization observed previously by our lab was observed in both skin inflamed for 18 and 72 hours in the present study though the present study found decreases in median mechanical thresholds of C/Aδ units while previous findings only found significant changes in C-fibers (Wenk et al., 2006). Discrepancies between these two findings could be due to the increased number of Aδ and C/Aδ-fibers studied in the present study. One interesting findings was that Aδ and C-fibers had lower median mechanical thresholds 18 hours after inflammation compared to 72 hours after inflammation, suggesting modulation of response properties between early and late stages of inflammation. These findings differ from another study that found no changes in mechanical thresholds or thermal thresholds between normal and CFA-inflamed skin using an *in vitro* glabrous skin-nerve preparation (Du et al., 2003). Fibers innervating inflamed skin were more likely to have spontaneous activity than units innervating normal skin. The percentage of spontaneous fibers between to two inflammatory stages did not differ except for C/Aδ units that had an increased percentage of spontaneous fibers in 72 hour inflamed skin. Taken together, fibers innervating inflamed skin demonstrate signs of sensitization.

Peripheral Opioid Receptors

It has been well documented that peripherally delivered opiates attenuate hyperalgesia following inflammation through their actions at MOR, DOR, and KOR (Ferreira and Nakamura, 1979; Joris et al., 1990; Stein et al., 1989). Our lab has previously provided electrophysiological evidence for functional opioid receptors on the terminals of primary afferent fibers 18 hours after CFA inflammation (Wenk et al., 2006). Using an *in vitro* glabrous skin-nerve preparation our lab showed that morphine, a non-selective opioid agonist, attenuated responses to both mechanical and thermal stimuli in a concentration-dependently and naloxone reversible manner suggesting these effects were receptor-mediated. Morphine has affinity for MOR at concentration in the lower nanomolar range but has affinity for DOR and KOR in the higher nanomolar and micromolar range. A range of concentrations was tested and the estimated EC_{50} or mechanical responses was 426 nM meaning the concentrations of morphine used in the study could have been acting on multiple opioid receptors. All three opioid receptors have been localized to peripheral cell bodies of primary afferent fibers under normal conditions (Arvidsson et al., 1995; Ji et al., 1995, Wang and Wessendorf, 2001), as well as on peripheral axons in normal skin (Coggeshall et al., 1997, Hassan et al., 1993; Pare et al., 2001; Wenk and Honda, 1999, Stein et al., 1989).

Our lab next sought to determine which opioid receptor was responsible for morphine's effects. Again using the *in vitro* glabrous skin-

nerve preparation, our lab evaluated the effects of the DOR-selective agonist deltorphin II on mechanical response properties of primary afferent neurons in 18-hour CFA-inflamed skin. Deltorphin II significantly decreased the excitability of C and C/Aδ-fibers in a concentration-dependent manner. These effects were blocked by the DOR selective antagonist naltrindole providing pharmacological evidence that these effects were mediated by DOR. These findings were consistent with earlier studies that showed DOR-selective agonists increase nociceptive thresholds of CFA-inflamed animals in the paw pressure test (Stein et al., 1989; Antonijevic et al., 1995; Zhou, 1998).

In the present study, the effect of the MOR-selective agonist DAMGO on mechanical excitability of primary afferent fibers evaluated was evaluated in skin inflamed for 18 hours. DAMGO was directly applied to the cutaneous receptive fields identified nociceptors. As a population, no significant changes in mechanical responses were observed suggesting that MOR is not involved with morphine's effect on neuronal excitability 18 hours after CFA inflammation. Two out of 32 units showed decreased responsiveness to suprathreshold mechanical stimuli.

One interesting observation that needs to be further studied is that 8 units (25%) demonstrated bursting activity ten to 20 minutes after drug application that last approximately two minutes. The origin of this activity is unclear. Based on the time it took for bursting activity to occur, it is possible that the drug was acting on receptors residing on other peripheral tissues leading to a release of compounds that resulted in excitability of these fibers.

Next, the present study addressed whether changes in opioid receptor regulation and/or availability occur between early and late stages on CFA inflammation. Three days after CFA injection was chosen as the late stage of inflammation due to findings that there are changes in MOR synthesis and trafficking at this time. First, the effects of morphine were evaluated in 72 hour inflamed skin to determine whether similar attenuation of mechanical responses would occur at this time. Direct application of morphine to the receptive field of identified nociceptors reduced mechanical responsiveness. In our earlier study, 58% of units studied had attenuated responses after morphine application. The present study only found 31% had attenuated responses. This could be due to changes in the testing protocol and to the addition of more Aδ and C/Aδ units though it must be noted that no significant change in responses between fiber-type was observed.

To determine whether the activation of MOR alters mechanical responsiveness in a skin inflamed for 72 hours, DAMGO was directly applied to the cutaneous receptive field of identified nociceptors. Substantial changes between 18 hour inflammation and 72 hour inflammation was observed. While DAMGO had no significant effect on the excitability of neurons in skin inflamed for 18 hours, it significantly reduced mechanical responsiveness of nociceptors innervating skin inflamed for 72 hours. The inhibitory effects were concentration-dependent and blocked by the nonselective antagonist naloxone providing pharmacological evidence that the effects were receptor-mediated.

Increased Efficacy of Peripheral Opioid Receptors

Our previous study and the present study demonstrated that the effects of peripherally administered opiates are enhanced under inflammatory conditions. Neither morphine nor DAMGO had an effect on neuronal excitability on units innervating normal skin. Morphine attenuated mechanical and thermal responses of units innervating 18 hour inflamed skin and reduced mechanical excitability of units innervating 72 hour inflamed skin. DAMGO did not alter mechanical excitability of units innervating 18 hour inflamed skin but significantly reduced mechanical responses to units innervating 72 hour inflamed skin suggesting a change in receptor availability or efficacy.

Several mechanisms may be involved for enhanced opioid receptor function under inflammatory conditions. The normally impermeable perineurial sheath that surrounds peripheral nerve fascicles may become disrupted following changes in osmolarity during inflammation, allowing more receptor ligand to bind to available receptors (Antonijeviz et al., 1995). It is also possible that proinflammatory mediators released during inflammation may also lead to perineurium breakdown.

Access of endogenous ligand could also account for increased receptor function. Endogenous ligands for all three opioid receptors, as well as the precursors preproenkaphalin and proproopiomelanocortin are packaged in infiltrating immune cells (Stein et al., 1990,1992; Brack et al., 2004). The presence of ligand may lead to receptor trafficking from internal stores to the plasma membrane (Coggeshall et al., 1997; Cahill et al., 2001).

Though opioid receptors are present on peripheral cell bodies and axons under normal skin, early inflammatory events may change the functional state or availability of existing receptors. It is unlikely that at early time points of inflammation (18 hrs) increased receptor synthesis and transport is responsible for increased opioid receptor efficacy though could account for changes observed between early and late stages for MOR. Consistent with this, increases in radiolabeled beta-endorphin binding in sciatic nerve is observed 24 hours after CFA inflammation (Hassan et al., 1993) as well as increases in MOR synthesis in dorsal root ganglion cells (Shaqura et al., 2004). Additionally, increases in immunohistochemical labeling of MOR is observed within 4 days of CFA injection (Stein et al., 1990). It is possible that changes in MOR function seen at 73 hours are due to increased receptor synthesis and trafficking.

Another possible reason that MOR function is enhanced at 72 hours is due to complex regulatory changes during exposure to ligand or due to interaction with other receptor-mediated events. Bradykinin is a proinflammatory mediator that is released during inflammation. It acts on two classes of G-protein coupled receptors B1 and B2. Activation of B2 by bradykinin can induce membrane insertion of intracellular DOR and induce functional competence (Patwardhan et al., 2005). Chemokines may also modulate opioid receptor function through coupling (Parenty et al., 2008). These findings suggest that opioid receptor function can be regulated through the mechanisms of other G-protein coupled receptors.

The present experiments demonstrate that MOR is differentially regulated during early and late stages of inflammation. DAMGO did not alter the neuronal excitability of units innervating skin inflamed for 18 hours (early stage) but did significantly reduce mechanical responsiveness of units innervating skin inflamed for 72 hours (late stage). Furthermore, neither morphine nor DAMGO altered response properties in units innervating normal skin but attenuated responses in units innervating inflamed skin.

Table 1

Units innervating skin inflamed for 18 hours

Unit type	#	Mean conduction velocity (CV)	Spontaneous	Nociceptor	Median mechanical threshold (mN)
Aδ	5	7.60 ± 2.67 m/s	2 of 5 (40%)	100%	37.74 (n=2)
C/Aδ	9	2.27 ± 0.34 m/s	2 of 9 (22%)	100%	10.00 (n=7)
C	18	0.91 ± 0.23 m/s	6 of 18 (33%)	100%	18.24 (n=4)

Units innervating skin inflamed for 72 hours

Unit type	#	Mean conduction velocity (CV)	Spontaneous	Nociceptor	Median mechanical threshold (mN)
Aαβ	1	18.1 m/s	0%	0%	n/a
Aδ	17	7.46 ± 2.9 m/s	6 of 17 (35%)	100%	14.55 (n=6)
C/Aδ	22	2.53 ± 0.4 m/s	9 of 22 (41%)	100%	10.00 (n=4)
C	49	0.91 ± 0.27 m/s	19 of 49 (39%)	44 of 49 (90%)	37.74 (n=10)

Units innervating normal skin

Unit type	#	Mean conduction velocity (CV)	Spontaneous	Nociceptor	Median mechanical threshold (mN)
Aαβ	3	19.1 ± 2.5 m/s	0%	0%	4.08 (n=2)
Aδ	13	10.3 ± 2.1 m/s	3 0f 13 (23%)	8 of 13 (62%)%	63.29 (n=7)
C/Aδ	11	2.8 ± 0.48 m/s	2 of 11 (18)%	9 of 11 (82%)	18.24 (n=9)
C	11	1.0 ± 0.43 m/s	1 of 11 (9%)	100%	82.50 (n=7)

Table 1: Distribution of single units

Thirty-two units were included in the study of skin inflamed for 18 hours after CFA. Of these, 5 conducted within the Aδ range with a mean CV of 7.60 ± 2.67 m/s, 9 units had conduction velocities within the C/Aδ range with a mean CV of 2.27 ± 0.34 m/s, and 18 units conducted in the C range with a mean CV of 0.91 ± 0.23 m/s. All units were functionally classified as nociceptive units based on their stimulus-response relationship. Forty percent of Aδ-fibers met the criteria for spontaneous activity while 22% of C/Aδ-fibers and 33% of C-fibers. Furthermore, all classifications of fibers demonstrated reduced mechanical thresholds.

Eighty-nine units were included in the study of skin inflamed for 72 hours. Of these, 17 conducted within the Aδ range with a mean CV of 7.46 ± 2.9 m/s, 22 units had conduction velocities within the C/Aδ range with a mean CV of 2.53 ± 0.4 m/s, and 49 units conducted in the C range with a mean CV of 0.91 ± 0.27 m/s. One hundred percent of Aδ and C/Aδ units were classified as nociceptors and 44 of 49 (90%) of C units were nociceptors. Thirty-nine percent of Aδ, 41% of C/ Aδ and 39% of C-fibers were spontaneously active. The median mechanical threshold for all three fibers types showed reduced mechanical thresholds compared to fibers innervating normal skin. One Aβ unit with a conduction velocity of 18 m/s was also included.

Thirty-eight fibers were tested that innervated normal skin. Mean conduction velocities did not differ between normal and inflamed skin. Fewer units innervating normal skin were classified as nociceptors or demonstrated spontaneous activity compared to units innervating inflamed skin.
Values are expressed as mean ± standard error (SEM)

Figure 1

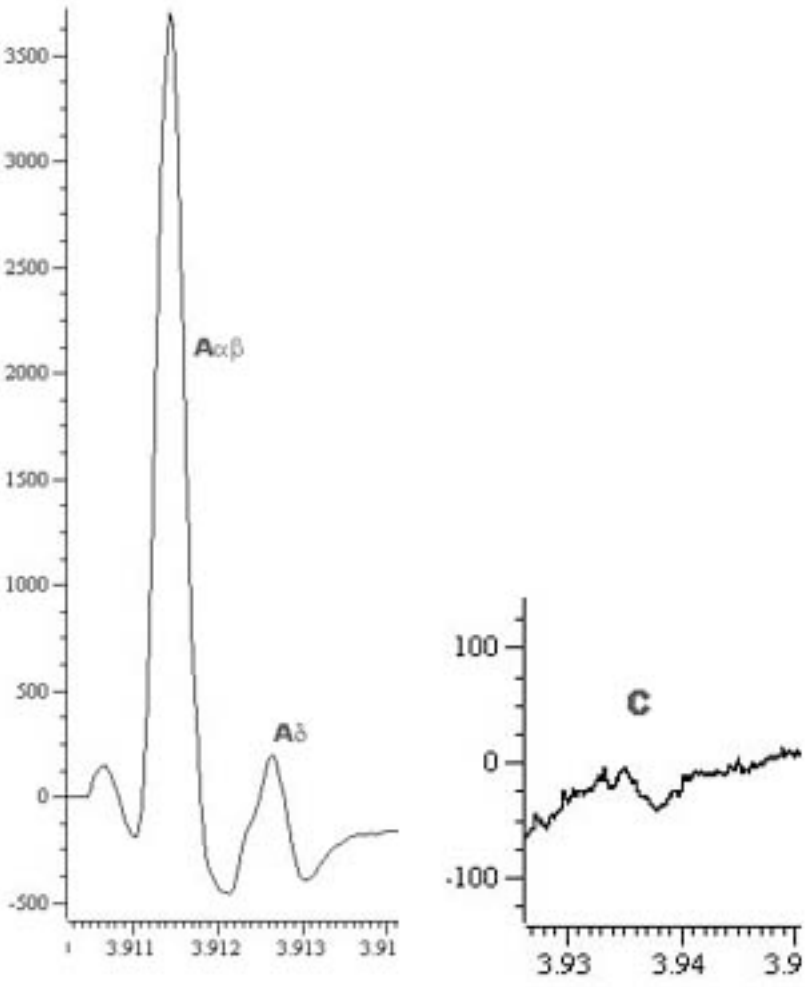
3500
3000
2500
2000
1500
1000
500
0
-500
Aαβ
Aδ
3.911
3.912
3.913
3.91
100
0
-100
C
3.93
3.94
3.9

Figure 1: Classification of single units by conduction velocity

This is a representative example of a compound action recording. There was no difference between compound action potential recordings taken from 18 hour inflamed skin and 72 hour inflamed skin so the data was combined. The Aαβ waveform had a mean conduction velocity of 29.2 ± 7.0 m/s with a mean range of 50.3 ± 15.0 m/s and 17.1 ± 4.2 m/s. The Aδ waveform had a mean conduction velocity of 10.3 ± 2.9 m/s with a mean range of 16.1 ± 3.3 m/s and 5.6 ± 2.6 m/s. The C waveform had a mean conduction velocity of 0.82 ± 0.2 m/s with a mean range of 1.10 ± 0.2 m/s and 0.70 ± 0.1 m/s. Units that had conduction velocities between the Aδ and C waves (3 and 1.7 m/s) were assigned to a C/Aδ group. All values expressed as mean ± sem.

Figure 2

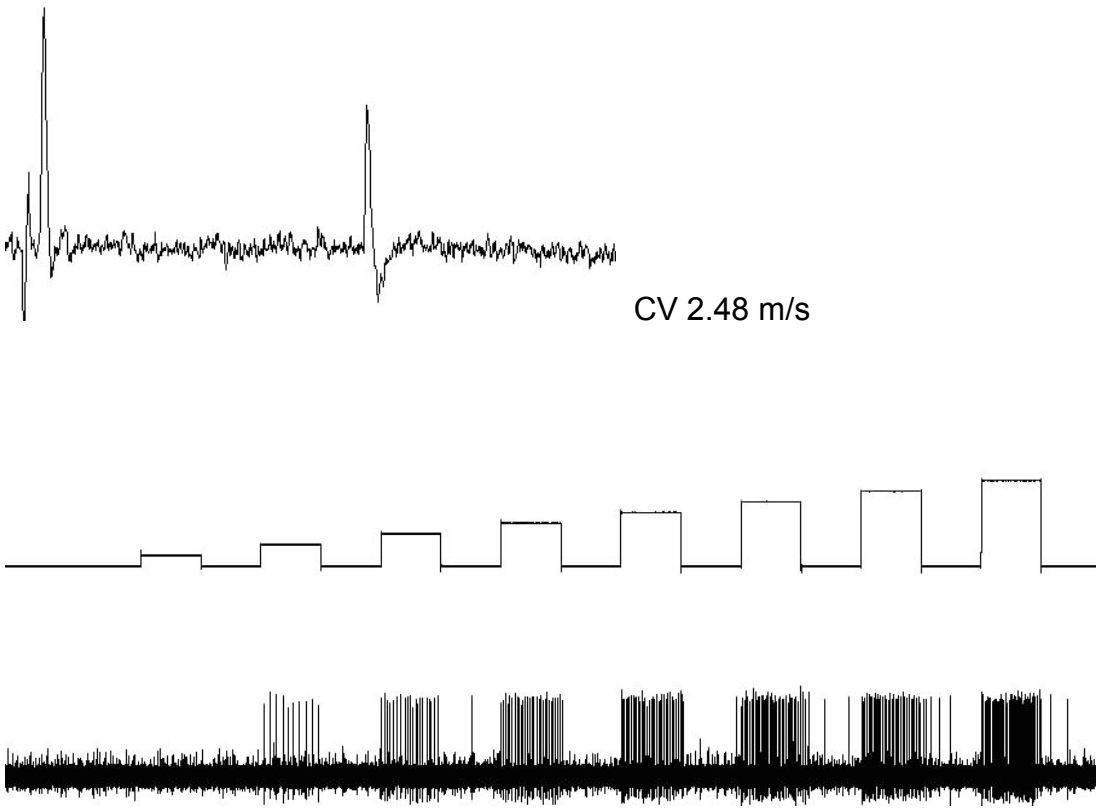

Figure 2: Classification of single units by mechanical stimulation

This is a representative example of graded mechanical stimulation to the cutaneous receptive field of a single C-fiber using a computer controlled probe. A unit was classified based on its stimulus-response relationship. A nociceptor was defined as a unit whose firing rate increased monotonically with increasing pressure of stimulation.

Figure 3

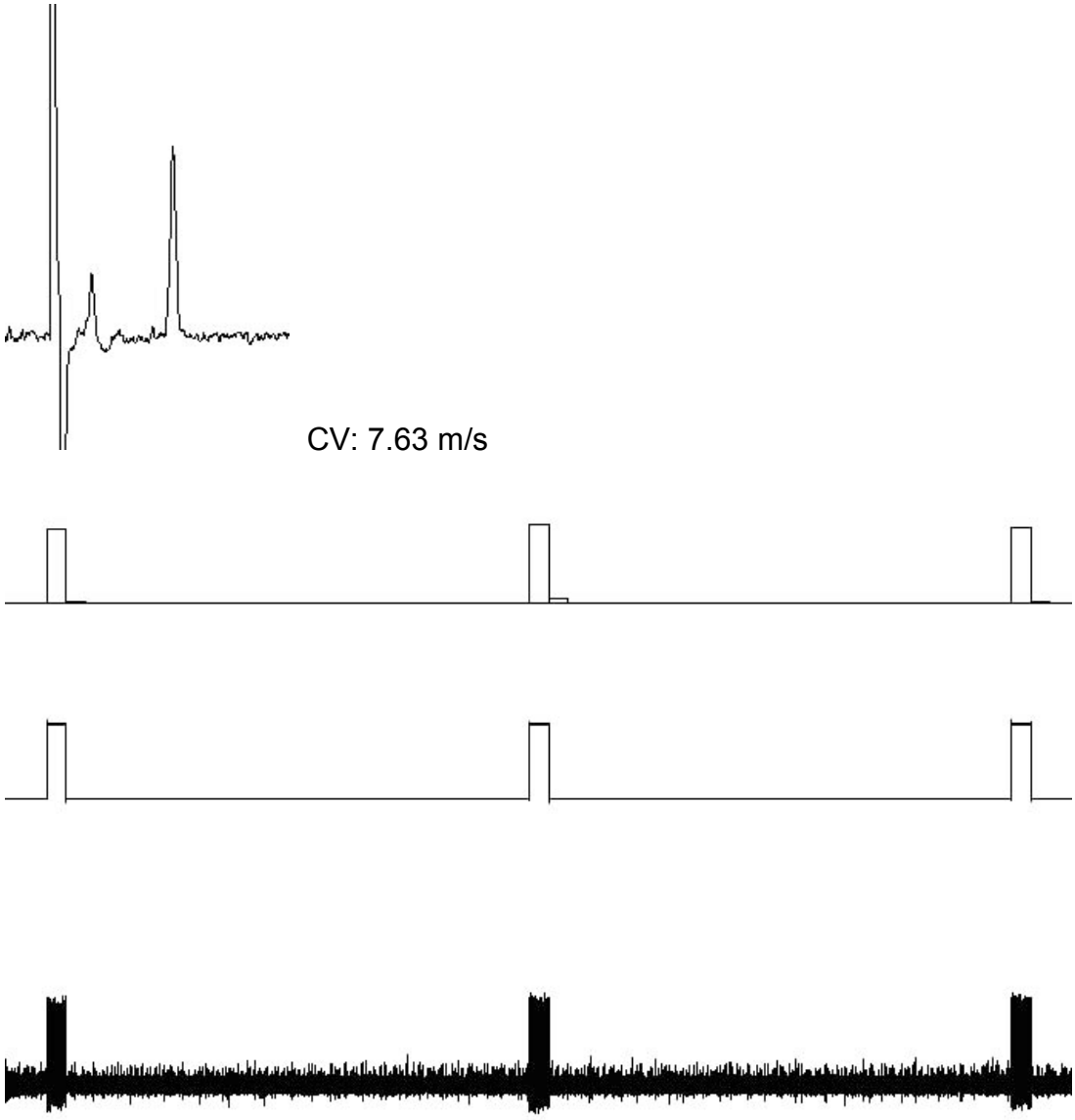

Figure 3: Reproducibility of responses to repeated mechanical stimulation

In order to differentiate drug effect from normal variability, 2 to 3 mechanical stimulations were recorded for before drug testing in order to calculate a baseline response (number of spikes). The ratio of spikes between BL 1 and BL 2 was measured and the ratio of spikes between BL 2 and BL 3. The average BL ratio was then measured. The ratio of BL 1 and BL 2 was used as the average if only two BL measurements were obtained.

Above is a representative example of repeated mechanical stimulations showing the recorded action potential (bottom), pressure trace (middle) and histogram (top) showing the rate of firing in 5 secs. Mechanical stimulation was produced using a computer controlled mechanical probe for with a duration of 5 seconds every 2 minutes. The values were used to measure baseline response to mechanical stimulation and calculate variability of repeated stimulation. The mean BL spike ratio of all units was 1.00 ± 0.14%. A positive drug response was considered a response falling above or below 2 standard deviations from the mean baseline (greater than 128% of less than 72% of baseline).

Figure 4

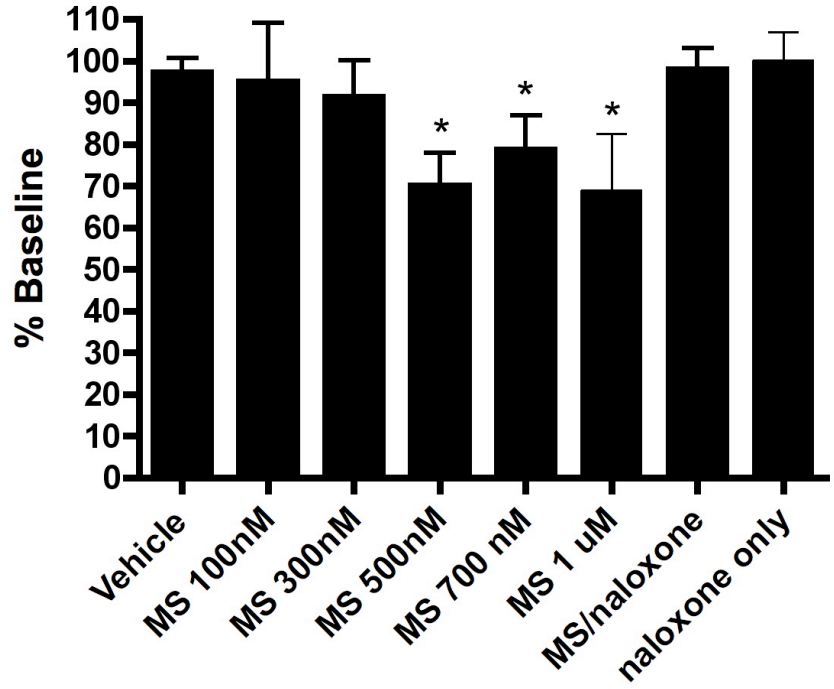
% Baseline
110
100
90
80
70
60
50
40
30
20
10
0
*
*
*
Vehicle
MS 100nM
MS 300nM
MS 500nM
MS 700 nM
MS 1 uM
MS/naloxone
naloxone only

Figure 4: Morphine sulphate decreased neuronal excitability: Population

Morphine sulphate reduced mechanical responses in isolated fibers from skin inflamed for 72 hours at concentrations of 500 nM, 700nM and 1 μM with mean percent baseline responses of 70.1 ± 7.8%, 78.6 ± 8.4%, and 68 ± 13.9% respectively. Vehicle treated fibers had a mean percent baseline response of 97.1 ± 3.6%. This effect was blocked by the morphine selective antagonist naloxone. To test if a basil level of endogenous opioid action is present in inflamed skin, naloxone was applied to the receptive field of 3 units. Naloxone applied alone did not alter mechanical responses.
The concentrations of morphine sulphate tested were: 100 nM (n=4), 300 nM (n=9), 500 nM (n=22), 700 nM (n=9), and 1 μM (n=7). Values are expressed as mean ± sem. (1-way ANOVA with Bonforoni post hoc tests, $p > 0.05$).
* compared to Vehicle

Figure 5

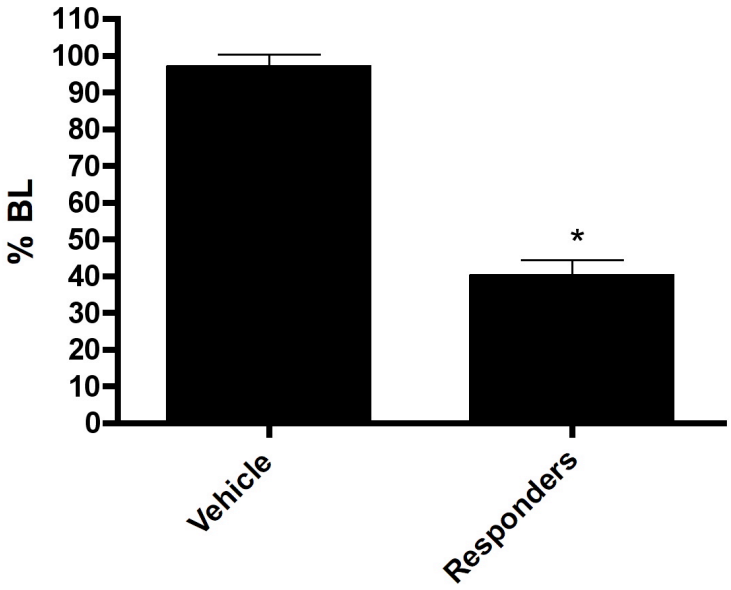

Figure 5: Morphine sensitive units

Morphine reduced responsiveness to noxious stimuli in 31% of all units treated with a mean percent baseline response of 39.99 ± 4.5% compared to 96.7 ± 3.6% for vehicle treated fibers. (*t*-test, $P > 0.05$).

Figure 6

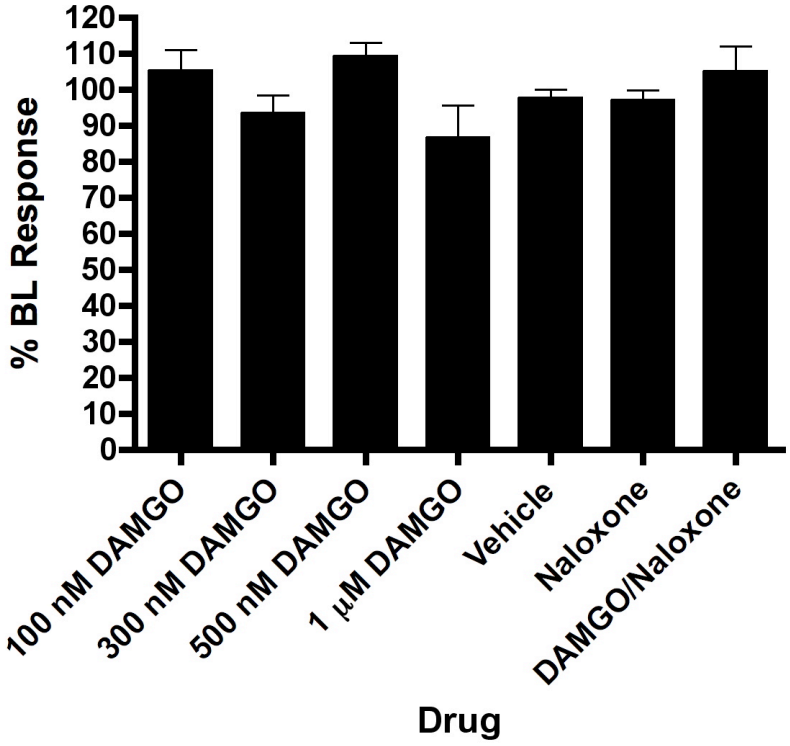
% BL Response
120
110
100
90
80
70
60
50
40
30
20
10
0
100 nM DAMGO
300 nM DAMGO
500 nM DAMGO
1 μM DAMGO
Vehicle
Naloxone
DAMGO/Naloxone
Drug

Figure 6: DAMGO does not significantly alter mechanical responses of fibers innervating skin 18 hours after CFA inflammation

A total of 23 units were tested with the following concentrations of the morphine selective agonist DAMGO: 100nM (n=6), 300nM (n=5), 500nM (n=4), and 1 μM (n=8). Population data for all concentrations of DAMGO did not significantly differ from vehicle treated fibers. (1-way ANOVA).

Figure 7:

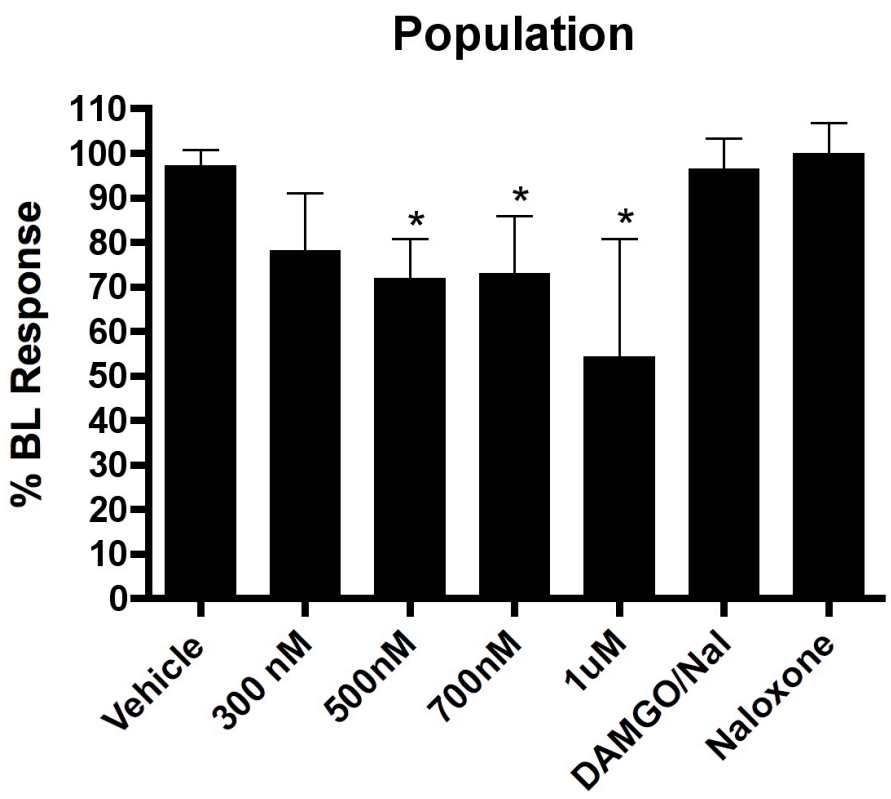
Population
% BL Response
110
100
90
80
70
60
50
40
30
20
10
0
*
*
*
Vehicle
300 nM
500nM
700nM
1uM
DAMGO/Nal
Naloxone

Figure 7: DAMGO decreased neuronal excitability of single units innervating skin inflamed for 73 hours

A total of 21 units were treated with the following concentrations of DAMGO: 100 and 300 nM (n=4), 500 nM (n=8); 700 nM (n=6), 1 μM (n=3). Mechanical responses of units treated with 500 nM, 700 nM and 1 μM were significantly reduced following morphine application with the following mean percent responses, 71.71 ± 9.1%, 72.84 ± 13.0%, and 54.16 ± 26.5% respectively compared to vehicle treated fibers (97.1 ± 3.6%). Co-application of 500 nM DAMGO + 1 μM naloxone blocked DAMGO's effect. (1-way ANOVA with Bonforoni post hoc tests, $p > 0.05$).

Figure 8

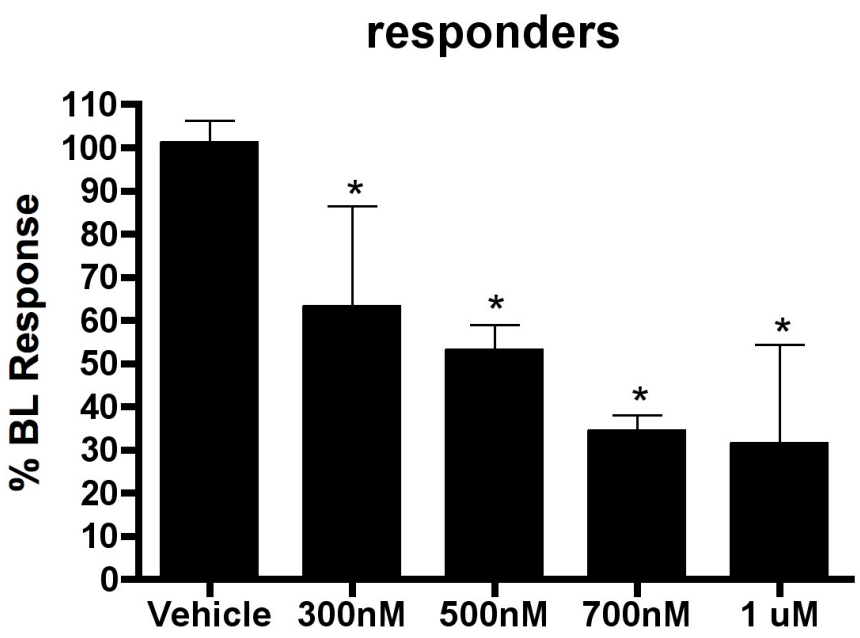
responders
% BL Response
110
100
90
80
70
60
50
40
30
20
10
0
*
*
*
*
Vehicle
300nM
500nM
700nM
1 uM

Figure 8: DAMGO sensitive units: 72 hours inflammation

Application of DAMGO (300 nM - 1μM) applied directly to the receptive fields of single sensory units innervating skin inflamed with CFA for 72 hours reduced responsiveness to noxious mechanical stimulation in a concentration dependent manner. Units included met criteria for a positive drug effect followed by a return to a least 50% baseline. No vehicle treated fibers met the criteria but is included as a comparison. The following data points were obtained: 300 nM (n=2), 500 nM (n=4), 700 nM (n=2) and 1 μM (n=2) with mean percent baseline responses of 62.9 ± 23.5%, 52.8 ± 6.2%, 34.3 ± 3.8%, and 31.3 ± 23.2% respectively. Mean percent response for vehicle treated animals was 97.1 ± 3.6%. (1-way ANOVA with Bonforoni post hoc tests, $P > 0.05$).

Figure 9

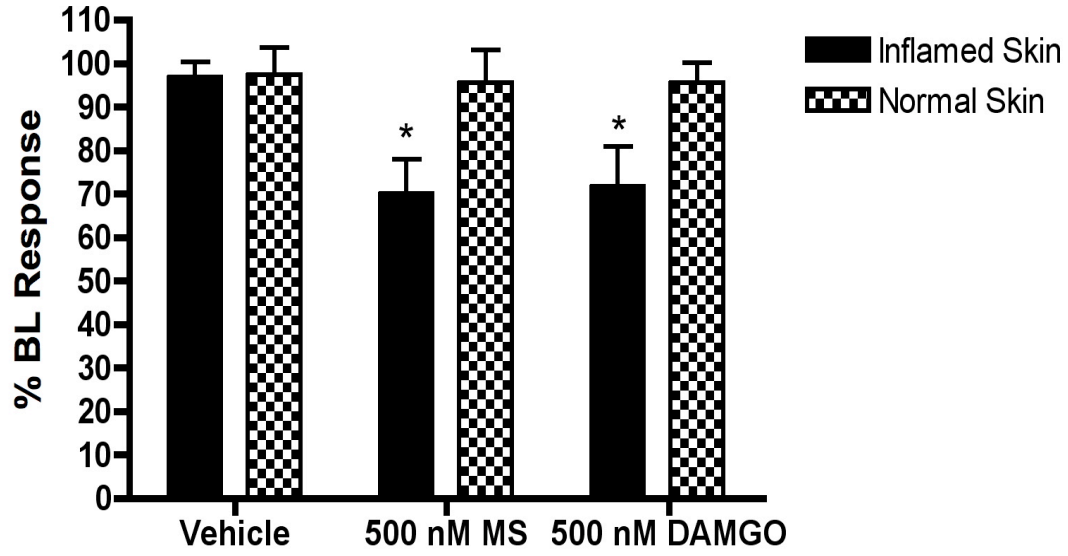
% BL Response
110
100
90
80
70
60
50
40
30
20
10
0
*
*
Vehicle
500 nM MS
500 nM DAMGO
Inflamed Skin
Normal Skin

Figure 9: Opiates reduce mechanical responses in skin inflamed for 72 hours but not normal skin

Neither morphine nor DAMGO had an effect on mechanical responses in normal skin but both significantly reduced responses in inflamed skin. All units treated with morphine and DAMGO (population) are displayed. Mean percent baseline responses after morphine in healthy skin (95.5 ± 7.4%) and inflamed skin (70.1 ± 7.8%). Mean percent baseline responses after DAMGO in healthy skin (95.4 ± 4.7%) and inflamed skin (71.7 ± 9.1%). Responses to mechanical stimulation were not significantly changed following vehicle application in healthy or inflamed skin. (1-way ANOVA with Bonforoni post hoc tests, $p > 0.05$).

* compared to vehicle

Chapter 3

UVB Irradiation: Characterization of a New Model for Cutaneous Hyperalgesia

Introduction

Living organisms have adapted overtime to utilize the electromagnetic energy emitted from the sun. These wavelengths include both visible light (390-700 nm) and ultraviolet (UV) radiation (290-400nm). UV radiation is further divided into three categories based on wavelength; long wave UVA (320-400nm), medium wave UVB (290-320nm), and short wave UVC (100-290nm). While most UVC radiation is absorbed by the earth's ozone layer, both UVB and UVA radiation reaches the earth's surface and penetrates the skin to varying degrees, with both beneficial and detrimental effects.

The effects of UV radiation overexposure on human skin have been well documented (Young et al, 1985; Harrison and Young, 2002) and include sunburn, cell damage, photoaging, and inflammation. The mechanisms of UVR-induced peripheral inflammation are not completely understood though there is increasing evidence that cutaneous sensory fibers may play a role through the release of neuropeptides and neurotransmitters. Additionally. UV irradiation can lead to sensitivity to both mechanical and thermal stimuli. A variety of inflammatory conditions can induce hyperalgesia and lead to sensitization of primary afferent fibers and it is of clinical importance to understand the underlying mechanisms leading to this altered state.

Acute skin over-exposure to UVR has recently been proposed as an inflammatory pain model in both rats and humans (Hoffman and Schmelz, 1999; Davies et al., 2005; Bishop et al., 2007; Saade et al., 2008). Many

commonly used persistent inflammatory animal models (Complete Freund's Adjuvant (CFA), carraggenan, zymosan) rely on the injection of antigen resulting in large-scale nonselective innate immune responses and the subsequent activation and recruitment of acquired immune systems. UVA and UVB radiation should be studied individually due to differences in their biological effects. Furthermore, UVA and UVB radiation penetrate the skin's surface to varying degrees thus the structures affected and the types of changes elicited differ. UVA radiation penetrates deep into the dermis while UVB radiation is mainly absorbed within the epidermal layers of the skin.

UVB-induced inflammation results mainly from apoptosis of epidermal cells and the release of pro-inflammatory agents. This type of injury has previously been described as a sterile injury (Bishop et al., 2007) and resulting inflammation may differ from models based on the addition of foreign material. A well-characterized UVB model of inflammatory pain could provide a needed translational pain model.

The aim of the present study is to develop and characterize a new UVB model of inflammation produced by a single exposure of the glabrous skin of the rat's hind limb to UVB light and to compare it to the commonly used CFA persistent inflammatory model of inflammation.

Methods

All experimental procedures were approved by the Institutional Animal Use and Care Committee at the University of Minnesota and conform to established guidelines.

Induction of Inflammation

Complete Freund's Adjuvant (CFA

Animals were briefly sedated with isofluorane before receiving a subcutaneous injection of 100 μl of CFA (1:1 emulsion in phosphate buffered saline, Sigma; St. Louis, MO) using a sterile 0.5 ml syringe into the right hindpaw.

UVB irradiation

Rats were deeply anaesthetized with isofluorane and placed on their stomachs and shrouded with a UV opaque material with only the plantar surface of the right hindpaw exposed, perpendicular to the narrowband UVB (Handisol, Amjo Corp, US) light source situated above. The narrowband UVB lamp emits a wavelength centered near 311nm. Irradiance produced by the bulbs during each session was determined at the distance of the limb from the light source using a calibrated meter UV340 Mannix UV light meter (General Tools & Instruments Company, NY, USA). UVB doses that rats were exposed to were calculated using the following formula:

Dosage Energy = UV intensity (constant measured by UV light meter) x time. UVB doses used were within the range of 60mJ/cm^2 to 500mJ/cm^2. Changes in doses was varied by varying time exposed to light wand.

Behavioral testing

Thermal sensitivity

Three separate groups were tested for thermal sensitivity to a radiant heat source. The first group consisted of five naïve rats that had not been exposed to either CFA or UVR. The second group consisted of two animals that had their right foot injected with CFA. The third group consisted of three animals that had their right foot exposed to a dose of 350mJ/cm^2 UVB light. All animals were acclimated to the testing procedure for three consecutive days prior to exposure to either CFA, UVB, or no exposure. Following the acclimation period, animals were tested at each of the following experimental time points: 1,4,24, 48, 72, 96, and 120 hours after exposure.

Heat sensitivity was determined by measuring withdrawal latencies in responses to radiant heat stimuli delivered to the plantar surface of both hind paws (Hargreaves et al.,988). Animals were placed individually on a glass platform in plexiglass chambers and allowed to acclimate for a minimum of 20 minutes. The temperature of the glass was maintained at 25 ± 1 °C. A radiant heat source was directed at the plantar surface of the hindpaw and the time for the rat react to the light beam was recorded as the withdrawal

threshold. Both paws were tested alternately at 5-min intervals for a total of 8 trials, 4 trials per foot. For each paw, the outlier (furthest from mean) was dropped and paw withdrawal latency was reported as the mean withdrawal latency of three readings. The heat source automatically shut off after a period of 20 seconds in order to avoid damaging the skin surface of unresponsive animals.

Mechanical sensitivity

Five separate groups of animals were tested for mechanical sensitivity using the up-down method previously described by Chaplan et al., 1994). The first group consisted of naïve rats that were not exposed to UVB light. The second group consisted of six animals that received a UVB dose of 60 mJ/cm^2 to the right hind paw. The third group consisted of six animals that received a dose of 80 mJ/cm^2 to the right hind paw. The fourth group of animals consisted of nine animals that received a UVB dose of 150 mJ/cm^2. The fifth group consisted of nine animals receiving a UVB dose of 350 mJ/cm^2. All animals were first acclimated to the testing the testing chambers and von Frey filaments for three consecutive days after which each animals was tested at each of the following experimental time points: 2, 4, 6, 8, 24, 48, 72, 96, 120, 144, 168, 192, 216, and 240 hours after UVB irradiation.

Mechanical sensitivity was tested using the up-down method with calibrated monofilaments (von Frey filaments). Animals were placed on a wire mesh platform in clear plastic cages and allowed to acclimate for a

minimum of 20 minutes. The 50% withdrawal threshold was determined using the Chaplan (1994) up-down method modified from Dixon (1980). The von Frey filaments were applied from underneath the platform perpendicular to the plantar service of the hindpaw until a slight bend occurred. A positive response was noted if the paw was withdrawn. Ambulation was considered an ambiguous response and in such cases the stimulus was repeated. Briefly, the testing regime started with a filament of 4.31g. Following a positive response, the next weaker stimulus was tested. In the absence of a response, a stronger stimulus was presented. This paradigm continued until a total of six measurements, including the one before the first paw-lifting response had been made, or until four consecutive positive or five consecutive negative (assigned a score of 15 g) responses had occurred. The resulting sequence of positive and negative responses was used to interpolated the 50% withdrawal threshold.

Measures of Inflammatory Response

Edema

Paw volume, a measure for edema, was determined using water displacement plethysmography. Six separate groups of rats were tested (Control, 60 mJ/cm^2; 150 mJ/cm^2; 350 mJ/cm2: 500 mJ/cm^2 , CFA n=3). Animals were lightly restrained in a plastic cone and the right hind limb was immersed in a small vessel containing room temperature water to a

standardized point (hairline) on the limb. The volume of water (mL) displaced was measured and the mean value of four trials was used for analysis. Data is expressed as volume (ml) ± sem.

Paw Temperature

Four separate groups of seven rats each were tested for changes in cutaneous temperature. The first groups consisted of naïve rats that did not receive UVR. The remaining three groups each received a dose of UVB radiation to the right hind paw (80 mJ/cm^2, 150 mJ/cm^2, or 350 mJ/cm^2). The temperature of the ipsilateral and the contralateral hind paw of each animal were measured at each of the following experimental time points: 6,12,24,48,72,96,120,144 and 168 hours after radiation.

Animals were lightly restrained in a towel and the skin surface temperature of each hindpaw was measured using a thermocouple. Temperature was reported as the mean of three readings taken a minimum of one minute apart.

Histopathological Measure of Inflammation

Glabrous skin from the right hind paw of six groups of animals was collected at four time points: 4, 48, 96, and 168 hours. Each group had two animals per time point. Group one consisted of naïve rats. Group two consisted of animals receiving a subcutaneous injection of CFA. Group three received a dose of 80 mJ/cm^2 UVB to the right hindpaw. Group four received

a dose of 150 mJ/cm^2 to the right hind paw. Group five received a dose of 350 mJ/cm^2 to the right hind paw.

Each animal received an overdose of Nembutal (IP). After reaching an areflexive state, the entire glabrous portion of the right hind limb was removed and immersion-fixed in 10% neutral-buffered formalin. Later, the footpads were removed and placed in 10% neutral-buffered formalin, cut along the midline/longitudinal axis of the footpad, and both halves processed into paraffin blocks using standard histology techniques. Histology slides were prepared by cutting 5 μm sections of tissue with a microtome, transferring onto glass slides and staining with hematoxylin and eosin; they were examined using light microscopy

Electrophysiological Studies

Glabrous Skin-Nerve Preparation

A glabrous rat *in vitro* skin-nerve preparation, described in detail for both hairy (Reeh, 1986) and glabrous skin (Du et al., 2001), was utilized to record from isolated sensory fibers innervating the glabrous skin of rat hindpaws. Rats were deeply anesthetized with a combination of ketamine, acepromazine and xylazine (6.8/0.09/0.45 mg/kg). The glabrous skin of the hindpaw was dissected and excised together with the attached tibial nerve and the medial and lateral branches of the plantar nerve. The skin-nerve preparation was immediately transferred to a chamber that was continuously

perfused (≥ 18 ml per minute) with warmed (30±2°C) oxygen-saturated synthetic interstitial fluid [SIF; containing in mM) 123 NaCl; 3.5 KCl, 0.7 $MgSO_4$, 2.0 $CaCl_2$, 9.5 Na gluconate, 1.7 NaH_2PO_4, 5.5 glucose, 7.5 sucrose, 10.0 Hepes; pH 7.45±0.05, 290±0.05 mOsm] (Koltzenburg et al., 1997). The preparation was placed corium side up in a chamber and anchored with insect pins. The preparation was further dissected until the skin and nerve were cleared of all tendons, muscles, and vasculature. The cut end of the tibial nerve was threaded through a small aperture into a second recording chamber and placed on top of a mirrored dissection platform. The recording chamber was filled with SIF buffer below and oil above the mirror.

Compound Action Potential

A compound action potential was recorded at the beginning of most experiments to assist in the classification of single units based on their conduction velocity. An insulated monopolar stimulation electrode was placed on the main trunk of the medial or lateral plantar nerve. Small filaments divided from the main tibial nerve were lifted onto a gold wire electrode with fine forceps for extracellular recording. The recording electrode was suspended in oil and referenced to the bath. Stimulating current was delivered with increasing intensity until each waveform component of the compound action potential (Aαβ, Aδ, and C) could be evoked. The rate of conduction measured for each waveform was expressed as meters per second. Electrical signals were amplified differentially (DAM80, World

Precision Instruments, Austin, TX), filtered, then routed in parallel to an oscilloscope and computerized data acquisition system (see below).

Isolation and Characterization of Single Units

Filaments were progressively divided and placed on the recording electrode until single unit activity could be isolated. Two search strategies were used to characterize single units. First, small bundles of nerve fibers were placed on the recording electrode, and a hand-held glass rod was used to gently probe for area of innervation on the corium surface of the skin. Second, an electrical search stimulus was used to isolate single fibers. A roving stimulating electrode was traced along the plantar nerve branches until the receptive field could be electrically identified. The stimulating electrode was positioned in the cutaneous receptive field and an electrically evoked spike was recorded to determine the latency from the stimulus to the spike. Distance was measured using thin suture placed along nerve. Conduction velocity was expressed as meters per second.

Spontaneous Activity

Unevoked baseline activity was recorded for at least 15 seconds before mechanical stimulation of the receptive field of each unit. Single units that had unevoked baseline activity greater that 0.1 spikes/second were classified as spontaneously active.

Characterization of Mechanical Response Properties

Mechanical response properties were determined using a combination of two methods. First, mechanical threshold was determined using calibrated von Frey filaments applied to the corium surface in order of increasing force. Filaments ranged from 0.5 mN to 96.5 mN. Threshold was defined as the lowest force capable of evoking at least two impulses.

Each probe was positioned with a micromanipulator and lowered onto the receptive field. Stimulus-response relationships were then determined for each unit. Responses were measured a computer controlled mechanical probe (Aurora Scientific Inc. Ontario, Canada) which a diameter of 1.2mm that produced a graded pressures (0.5–5.0 bars) for a duration of five seconds each. Nociceptors were defined as units whose firing rate increased monotonically with increasing pressure of stimulation. High threshold units that responded only to the maximal stimulus were also defined as nociceptors. The lowest force required to produce at least two impulses was reported as each unit's mechanical threshold. The stimulation onset and offset times were signaled to the online data acquisition program.

Characterization of Thermal Response Properties

Identified units were tested for thermal sensitivity. Initial experiments used heated SIF buffer applied directly to the corium through a small plastic ring (internal diameter 8mm) placed around the receptive field. Later, a 7 x 7 mm feedback controlled latex wrapped Peltier device applied to the corium

surface applied thermal stimuli. Thermal stimulation was delivered in a ramp (1°/sec) from a baseline of 30°C to a maximum of 50°C. Additionally, some units were tested for cold response using a ramp descending from 30°C to 0°C.

Data Collection and Analysis

Compound action potential and teased fiber recordings were collected using Spike 2 software (CED; Cambridge, UK). Data were analyzed on- and off-line. Offline data analysis was conducted using Spike 2. All values are expressed as mean ± standard error.

Results

General Observations

General skin appearance (redness, peeling, and formation of blisters) was monitored in both control and treated rats. Moderate redness became apparent 3-8 hours after exposure to UVB doses larger than 350 mJ/cm^2 and all changes subsided within 24 hours with the maximal dose used (500 mJ/cm^2). Minor peeling was observed five days after irradiation of doses over 150 mJ/cm^2. Skin blistering or lesions were not observed at the doses used. No significant changes were observed either in control animals or on the contralateral hind paw.

Behavior

Effect of UVB and CFA on Thermal Thresholds

The right hind paws of rats were either exposed to 350 mJ/cm^2 UVB light or injected with CFA. Five rats did not receive a treatment and were used as control animals. The contralateral and ipsilateral hind paws all animals were tested for thermal sensitivity at the following time points: 1,4,24, 48, 72, 96, and 120 hours after exposure.

UV exposure to the hind paw evoked significant ipsilateral thermal hyperalgesia (Figure 1) as early as 24 hours post –UVB. Withdrawal latencies did not return to baseline values for several days. Peak sensory changes were seen at 48 hours. At this time, mean withdrawal latency decreased to 4.5 ± 1.3 seconds for irradiated animals compared to the mean withdrawal latency of 9.6 ± 1.1 seconds for control animals. No significant difference was observed in contralateral hind paws.

CFA produced similar ipsilateral thermal hyperalgesia (Figure 1). Statistically significant hyperalgesia was produced as early as four hours post-injection and lasted several days. Peak changes were seen at 24 hours post-injection with a mean withdrawal latency of 4.4 ±0.6 seconds compared control animals (10.8 ± 1.4 seconds).

Effect of UVB on Mechanical Thresholds

The glabrous skin of rat hind paws was examined for changes in mechanical sensitivity following irradiation of UVB doses of 0,60, 80, 150, and 350 mJ/cm^2 (Figure 2). None of these animals developed noticeable blisters at these doses. Significant mechanical allodynia emerged following treatment with UVB doses of 80, 150, and 350 mJ/cm^2 showing a clear dose dependency. All three doses demonstrated peak sensory changes 72 hours post-UV exposure. The mean paw withdrawal threshold (PWT) were 9.5 ± 1.9, 6.0 ± 1.2, and 3.3 ± 0.7g, respectively, for UV doses of 80, 150, and 350 mJ/cm^2 compared to 14.9 ± 0.1g for animals receiving no (0 mJ/cm^2) UVB.

Physiological Studies

Effect of UVB on Edema

Edema is one hallmark of inflammation. Changes in paw volume were measured in order to determine whether CFA or UVB leads to swelling of the hind limb. The right hind limb of rats either received a subcutaneous injection of CFA or was irradiated with the following doses of UVB (0, 60, 150, 350, or 500 mJ/cm^2). Paw volume was measured one day before treatment to quantify baseline paw volumes and was later measured beginning at 2hrs post treatment to 216 hours post treatment. Values are expressed as mean paw volume of treated limb (mL). No changes in contralateral limb were apparent.

CFA produced significant swelling as early as 2 hours (Figure 3) peaking between 24 and 48 hours (2.4 ± 0.2 mL for both) compared to control animals at the same times (1.5 ± 0.0 mL). At this time the hind limb almost doubled in volume. The two highest doses of UVB (350 and 500 mJ/cm^2) produced significant swelling though not to the degree caused by CFA. A dose of 500 mJ/cm^2 UVB produced an increase in paw volume 48 hours after irradiation (1.9 ± 0.1 mL) compared to animal's receiving no UVB at the same time point (1.5 ± 0.0 mL). This subsided by 96 hours. A 300 mJ/cm^2 UVB dose caused a small but significant increase in paw volume 72 hours after irradiation (1.9 ± 0.0 mL) compared to animals receiving no irradiation (1.5 ± 0.0 mL) at this time.

UVB does not produce changes in skin temperature

Increases in temperature are seen during inflammatory conditions. Glabrous surface temperature was monitored before irradiation and 2 hours to 168 hours after irradiation. No significant change in paw temperature was observed following any dose of UVB. Average cutaneous temperature of the ipsilateral hind paw of control animals and rats receiving doses of 80, 150 and 350 mJ/cm^2 are as follows: 29.48 ± 0.2, 29.6 ± 0.1, 29.5 ± 0.1 and 29.6 ± 0.2 respectively.

Histology

Foot pads from the right hind limb of animals either receiving CFA or the following doses of UVB: 0 (control), 80, 150, 350, and 500 mJ/cm^2, were collected, fixed in 10% neutral buffered formalin, and prepared for histopathological investigation, for examination at 4, 48, 96 or 168 hours after treatment. A total of 40 animals were used (2 animals per treatment per time point).

Major differences between CFA and UVB were observed (summarized in Table 1). CFA caused severe inflammation as early as 4 hours after injection with moderate neutrophil infiltration in the dermis and severe dermal edema. Two days after CFA injection, poorly organized granulomatous inflammation was apparent along with severe edema (Figure 5). This continued for the duration of the study (168 hours) accompanied by the formation of severe granulomatous inflammation with a neutraphil component.

The lowest UVB dose studied (80 mJ/cm^2) did not produce any significant changes in the skin. 180 mJ/cm^2 produced only mild inflammation at 48 hours with the presence of mild intraepidermal vesicles and the presence of subcutaneous neurtrophils and mononuclear cells (Figure 5). The largest doses tested (350 and 500 mJ/cm^2) produced prominent damage at 48 hours. No significant findings were apparent at 4 hours but it is likely that inflammation could be apparent at earlier time points between 4 and 48 hours. At 48 hours, severe epidermal separation occurred with subepidermal vesiculation. Inflammation was accompanied by the infiltration of neurtrophils

and mononuclear cells into the epidermis. By 96 hours, similar findings were observed accompanied by epidermal crusting, subcorneal exudation, and increased cellularity of the dermis. Epithelial regeneration was also observed. These findings are consistent with a healing/reparative process (Figure 5). By day 7 (168 hrs), the tissue was almost completely repaired.

Electrophysiological Studies

Compound Action Potentials and Classification of Single Units by Conduction Velocity

Compound actions potentials were recorded at the beginning of most experiments from the tibial nerve of 27 animals (14 from normal animals and 13 from UVB irradiated animals) to be used to classify single units by conduction velocity (Figure 6). No significant difference was observed between compound action potentials recorded in normal skin and UVB irradiated skin and the values were combined.

The conduction velocity ranges of all three major wave components (Aβ, Aδ and C) are expressed as mean ± standard error (sem). The average mean conduction velocity for the Aαβ wave component was 27.9 ± 4.4 m/s and ranged from 60.2 ± 12.3 m/s to and16.6 ± 2.9 m/s. The Aδ wave had a mean conduction velocity of 11.9 ± 2.8 m/s and ranged from 16.5 ± 4.1 m/s

and 7.60 ± 1.9 m/s. The C wave had a mean conduction velocity of 0.84 ± 0.2 m/s and ranged from 1.09 ± 0.2 m/s to 0.59 ± 0.1 m/s.

The Aδ and C wave components did not overlap. The minimum conduction velocity for the Aδ wave was 3.4 m/s while the fastest C conduction velocity recorded was 1.6 m/s. Based on the above measurements, single units were classified as follows. Units with conduction velocities greater than 16.5 m/s were considered to conduct in the Aβ range. Those conducting between 16.5 m/s and 4.0 m/s were classified as Aδ units. Units conducting below 1.5 m/s were considered C fibers. Units that had conduction velocities that fell between the Aδ and C wave components of the compound action potentials (conducting between 4 and 1.5 m/s) were assigned to a C/Aδ classification.

Functional Classification of Single Units

A total of 68 units isolated from the tibial nerves of 27 rats was examined, 38 units from normal skin, and 30 from skin irradiated with 350 mJ/cm^2. The distributions of all primary afferent fibers are summarized in Table 2. Single units were assigned to the following categories based on their response properties: low-threshold mechanoreceptors (LTM), nociceptors, and thremoreceptors. Units classified as LTM responded only to mechanical stimulation, had a mechanical threshold in the lower bar range (< 3 bars), and did not display graded responses to increasing force displayed by nociceptive units. Nociceptors are units that respond preferentially to

noxious mechanical or thermal stimuli. Units were classified as nociceptors if their firing rate increased monotonically with increasing mechanical force or thermal stimulation. A computer controlled mechanical probe that produced a graded force between 0.5 and 5.0 bars was used to measure mechanical stimulus response relationships (Figure 7). A noxious level of force was determined to be 3 bars of pressure consistent with psychophysical studies reporting that pain thresholds start around 3 bars (Burgess and Perl, 1967; Hardy et al., 1952). A peltier device was used to deliver thermal stimulation as a ramp (1°/sec) from a baseline of 30°C to a maximum of 50°C. Some thermal responses were measured by adding heated SIF buffer to the receptive field. Additionally, some units were tested for cold response using a ramp descending from 30°C to 0°C. Earlier work in our lab determined that a noxious range of 35-43 °C on the corium surface corresponded to temperatures ranging from 40-48 °C on the epidermal surface of the preparation (Wenk et al., 2006). These thermal temperatures correspond to pain thresholds in psychophysical studies (LaMotte and Campbell, 1978). Nociceptors were further classified according to conduction velocity.

Thermoreceptors were classified based on thee following criteria: static discharge at baseline temperatures, responses to temperature changes with either a warming or cooling component and mechanical insensitivity or very high mechanical threshold (Hensel and Iggo, 1971).

Single Units Innervating Normal Skin Compared To Irradiated Skin

Spontaneous Activity

More units in irradiated skin displayed spontaneous activity compared to units innervating normal skin. Spontaneous activity was defined as a firing rate ≥ .1 spike/sec in the absence of applied stimulus. In normal skin, 9 of 38 (24%) units displayed spontaneous activity. Of these 2 of 11 (18%) was classified as a C-fiber, 2 of 11 (18%) were C/ Aδ-fiber units and 3 of 13 (23%) were classified as Aδ-fibers. In irradiated skin 15 of 30 (57%) units were spontaneously active, 13 of 14 (92%) were C-fibers, 1 of 6 (17%) were C/Aδ-fibers, 2 of 6 (33%) were Aδ-fibers, and 1 of 4 (25%) was an Aβ-fiber.

Mechanical Response Properties

All but two units studied responded to mechanical stimulation. One of these units was found in normal skin and classified as a C/Aδ-cold nociceptor and one unit innervating irradiated skin was classified as a thermoreceptor. The von Frey thresholds for 46 units (25 from normal skin, 21 from irradiated skin) were measured (Figure 8). The mean von Frey thresholds were significantly reduced for C-fiber units (2.7 ± 0.4 bars) and Aδ units (1.7 ± 0.4 bars) innervating irradiated skin compared to C and Aδ innervating normal skin (5.2 ± 1.1 and 4.5 ± 0.9 bars respectively). No significant difference was found between Aβ and C/Aδ units.

Thermal Responses of C-fibers

Units were tested for thermal responsiveness using either a peltier device or warmed SIF buffer applied to the receptive field. In normal skin, a total of 17 units were tested for thermal responses. Of the 10 units with thermal responses, 2 conducted in the Aδ range, 4 conducted within the C/δ range (plus 1 units that was mechanically insensitive but responded to cooling), and 3 conducted in the C range. A total of 11 units innervating irradiated skin were tested for thermal responsiveness. Of these, 7 units responded to thermal stimuli (1 Aδ-fiber unit, 5 C-fiber units). Heat thresholds did not differ between units innervating normal and irradiated skin (Figure 9)

Discussion

The objective of the present study was to characterize a UVB model of cutaneous hyperalgesia. The classic signs of inflammation are redness, pain, edema, heat, and sometimes loss of function. Changes in skin color were observed within the first hours after irradiation but no quantification of this was made. UVB irradiation resulted in pronounced thermal hyperalgesia with peak changes in paw withdrawal latency occurring 48 hours after exposure. This result is similar to hyperalgesia induced by CFA. UVB also produced dose-dependent mechanical allodynia. These findings are consistent with recent reports that demonstrated UVB-induced mechanical and thermal sensitivity in rats (Saade et al., 2008; Bishop et al., 2005).

Paw volume changes were assessed in order to determine whether swelling occurs following UVB irradiation. The largest doses, 350 and 500 mJ/cm^2 produced a significant increase in paw volume size 48-72 hours after exposure though it was not as pronounced as swelling produced from CFA injection. No changes in cutaneous temperature of the paw were found. It is unknown whether our probe was sensitive enough to detect possible temperature changes or if the thick epidermis found on the glabrous surface of the hind paw was too thick to detect small temperature changes. It is also possible that changes in skin temperature occurred before measurements were made. A recent study found small changes in skin temperature following UVB exposure that occurred between 1 and 2 hours (Saade et al., 2008).

Histopathological analysis was undertaken in order to determine the type and amount of inflammation produced by UVB and CFA. CFA produced pronounced inflammation as early as 4 hours and proceeded for 168 hours. Inflammation was localized to the dermis and was characterized by dermal edema, moderate to severe granulomatous inflammation and infiltration of neutrophils into the dermis. This is consistent with an immune response mounted for the destruction of foreign material. Damage caused by UVB irradiation was mostly localized to the epidermis, consistent with the idea that UVB rays are mainly absorbed by the epidermal layers of the skin. The type of inflammation produced differed greatly from CFA inflammation. Inflammation was not apparent at 4 hours, peaked around 48 to 72 hours,

and was almost completely gone by 168 hours. This is consistent with behavioral findings in this study as well as others that show hyperalgesia is prominent 24-72 hours after UVB exposure (Saade et al., 2008; Bishop et al., 2007) UVA exposure (Harison and Young, 2002; Harrison et al., 2004; Davies et al., 2005). Higher doses of UVB produced moderate to severe epidermal separation and in some cases the production of exudate was observed. Immune cell infiltration was mainly localized to the epidermis with an influx of a mixture of neutrophil and mononuclear cells. These findings, along with crusting of the epidermal surface, are consistent with a healing/reparative immune process.

To further characterize the UVB model, we examined whether UVB sensitizes primary afferent fibers using an *in vivo* skin-nerve preparation. Primary afferent fibers innervating irradiated skin had increased levels of spontaneous activity. Similar findings were reported in polymodal nociceptors exposed to broadband UV irradiation (Andreev et al., 1994) though one report did not observe increases in spontaneous activity (Bishop et al., 2007). UV-induced increases in baseline discharges of polymodal nociceptors have also been described (Eschenfelder et al., 1995; Szolcsanyi et al., 1987). Mechanical thresholds were measured using von Frey filaments. UVB resulted in reduced mechanical thresholds of C-fiber and Aδ-units. Previous work from our lab has demonstrated reduced mechanical thresholds of C-fiber units (Wenk and Honda, 2006).

The evidence for UVB induced inflammation and hyperalgesia correlates well with previously reported findings. Proinflammatory cytokine and NGF levels increase in irradiated hind paws at times consistent with behavioral hyperalgesia (Saade et al. 2008). Furthermore, UV leads to the release of histamine, substance P and CGRP (Legat et al., 2002; Eschenfelder et al., 1995; Hruza and Pentland, 1993) and increased levels of arachidonic acid and prostaglandins (Black et al., 1980; Gilchrest et al., 1981). These compounds are consistent with inflammatory conditions and have been shown to produce sensitization of primary afferent fibers similar to that demonstrated in this chapter (Dray and Bevan, 1993; Julius and Basbaum, 2001).

In conclusion, the present study characterizes a new model of UVB of cutaneous hyperalgesia. This model produces pronounced mechanical allodynia and thermal hyperalgesia as well as mild edema. These are all hallmarks of inflammation. Furthermore, the type of inflammation produced by UVB is localized to the epidermis and differs greatly from CFA-induced inflammation. This inflammation leads to the sensitization of nociceptors characterized by increases in spontaneous behavior and reduced mechanical thresholds.

Table 1

	4 HOURS	48 HOURS	96 HOURS	168 HOURS
80 mJ/cm^2	NSF	NSF	NSF	NSF
150 mJ/cm^2	NSF	**Transient** Inflammation: Mild intraepithelial vesicles, mixed immune cell	NSF	NSF
350 mJ/cm^2	NSF	**Severe Injury:** Severe epidermal separation, PMN and monos in epidermis and dermis	**Healing-Reparative Processes:** Moderate exudation, degen PMNs, mild dermal monos	**Almost Complete Healing:** Mild epidermal crusting, increased cellularity of dermis
500 mJ/cm^2	NSF	**Severe Injury:** Severe epidermal separation, PMN and monos in epidermis and dermis	**Healing-Reparative Processes:** Moderate exudation, degen PMNs, mild dermal monos, thinning of epidermis, increased cellularity of dermis	NSF
CFA	**Acute Inflammation:** Moderate PMN, severe dermal edema	**Severe Inflammation:** PMNs, poorly organized granulomatous inflammation	**Severe Inflammation:** PMNs, moderate granulomatous inflammation, MC	**Severe Inflammation:** PMNs, severe granulomatous inflammation

Abbreviations: degen- degenerated; MC- mast cells; monos- mononuclear cells; NSF- no significant findings; PMN- polymorphonuclear cells (neutrophils); subcut- subcutaneous

Table 1: Histopathological findings of UVB and CFA inflammation

There are major differences in the UV- and CFA-induced tissue responses.

The response to CFA predominantly involved the dermis with acute inflammation observed as early as 4 hours, progressing to poorly organized granulomatous inflammation at 48 hours, and sustained granulomatous response by day 7.

UV damage was not observed at 4 hours but was prominent at 48 hours. The UV-induced lesions predominantly involved the epidermis, in contrast to CFA that was associated with a dermal response. There also was early resolution of the UV-induced injury present around 96 hours, and almost complete resolution by day 7. These findings are consistent with a single, transient, but severe and dose-dependent injury induced by UV, in contrast to chronic, sustained injury caused by CFA.

Table 2

	NORMAL SKIN	IRRADIATED SKIN
Aβ	N=3 Nociceptive: 0% Spontaneous: 0% 3 LTM	N=4 Nociceptive: 0% Spontaneous: 1/4 (25%) 4 LTM
Aδ	N=13 Nociceptive: 10/13 (77%) Spontaneous: 3/13 (23%) 2 ADMH	N=6 Nociceptive: 3/6 (50%) Spontaneous: 2/6 (33%) 1 ADMH 1 LTM
C/Aδ	N=11 Nociceptive: 8/11 (72%) Spontaneous: 2/11 (18%) 1 C/ADC 4 C/ADMH	N=6 Nociceptive: 6/6 (100%) Spontaneous: 1/6 (17%)
C	N=11 Nociceptive: 9/11(82%) Spontaneous: 2/11 (18%) 3 CMH	N=14 Nociceptive: 13/14 (92%) Spontaneous: 11/14 (79%) 1 Thermoreceptor 3 CMH 1 CMHC
	Total: 38	Total: 30

Table 2: Summary of primary afferent fibers innervating normal and irradiated skin.

Summary of individual primary afferent fibers innervating normal and irradiated skin. Units are grouped by conduction velocity.
Abbreviations: ADMH: Aδ-mechanoheat nociceptive; CMH: C mechanoheat nociceptive; CMHC: C-mechanoheat-cold nociceptive; LTM: low-threshold mechanoreceptive

Figure 1

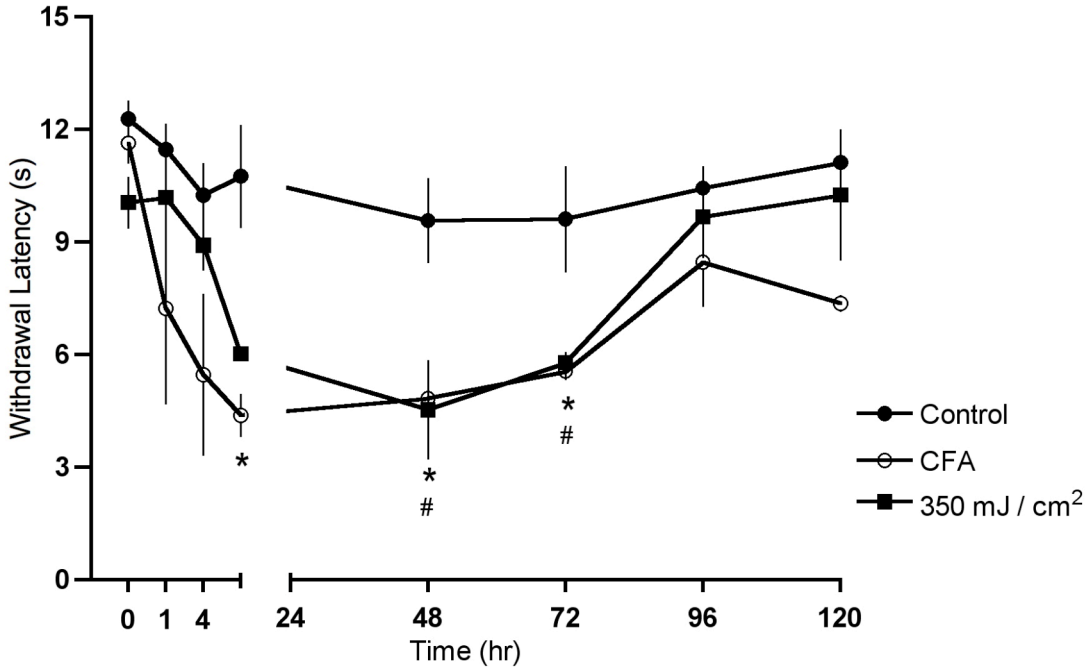
15
12
9
6
3
0
Withdrawal Latency (s)
0
1
4
24
48
72
96
120
Time (hr)
*
*
#
*
#
Control
CFA
350 mJ / cm2

Figure 1: UVB and CFA produces significant thermal hyperalgesia:

The right hind paws of rats were either exposed to 350 mJ/cm^2 UVB light, injected with CFA, received no treatment and tested for thermal sensitivity at the following timepoints: 1,4,24, 48, 72, 96, and 120 hours after exposure. Significant hyperalgesia was evident 24 hours following UVB exposure with peak sensitivity at 48 hours (mean withdrawal latency 4.5 ± 1.3 secs). CFA produced significant hyperalgesia as early as 4 hours with peak sensitivity at 24 hours (mean withdrawal latency of 4.4 ±0.6 secs).

* CFA; # 350 mJ/cm^2; ($p < 0.05$, two-way ANOVA)

Figure 2

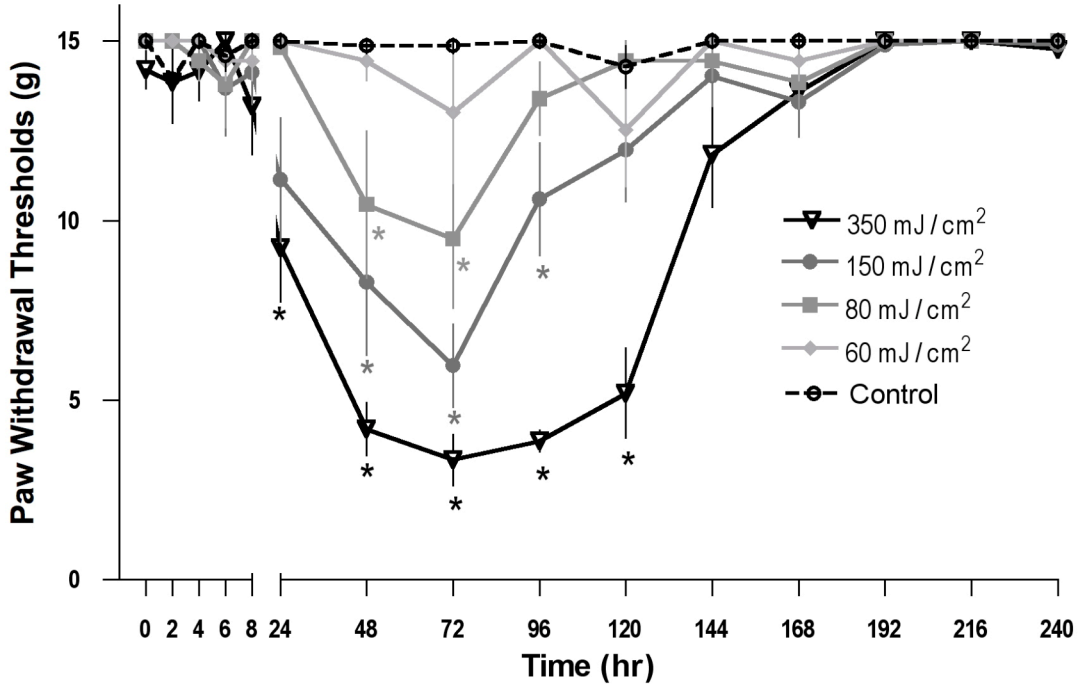
Paw Withdrawal Thresholds (g)
15
10
5
0
0 2 4 6 8 24 48 72 96 120 144 168 192 216 240
Time (hr)
350 mJ / cm2
150 mJ / cm2
80 mJ / cm2
60 mJ / cm2
Control
*

Figure 2: UVB exposure produces significant mechanical allodynia

The right hind paws of rats were exposed to the following doses UVB doses: 0 (n=8), 60 (n=6), 80 (n=6), 150 (n=9), and 350 (n=9) mJ/cm^2. UVB doses of 80, 150 and 350 mJ/cm^2 produced significant mechanical allodynia with peak sensory changes at 72 hours. ($p < 0.05$, two-way ANOVA)

Figure 3

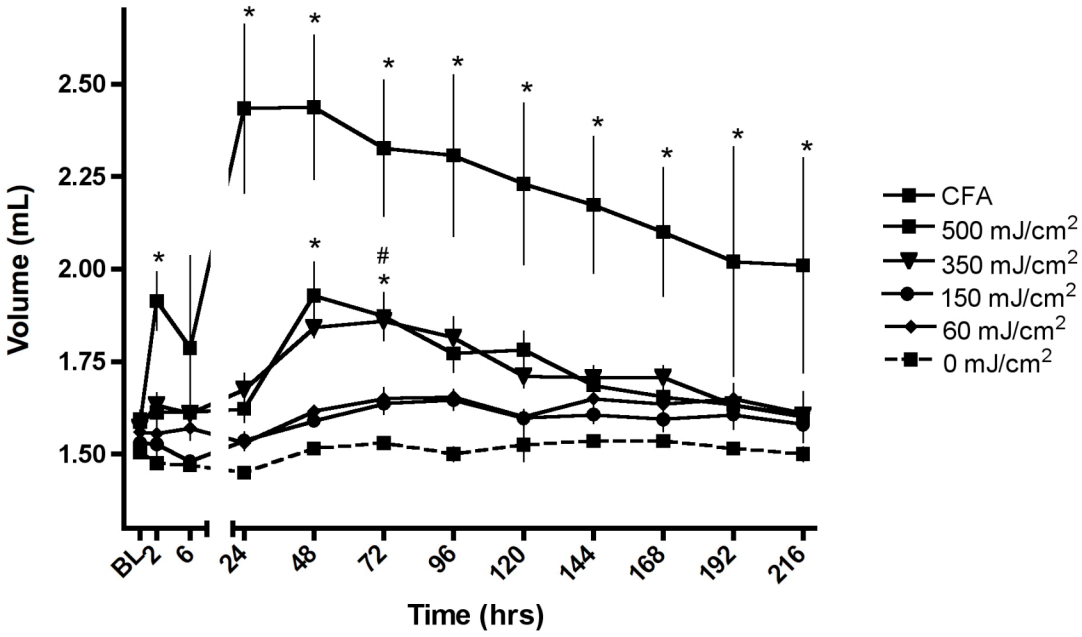
Volume (mL)
2.50
2.25
2.00
1.75
1.50
BL
2
6
24
48
72
96
120
144
168
192
216
Time (hrs)
CFA
500 mJ/cm2
350 mJ/cm2
150 mJ/cm2
60 mJ/cm2
0 mJ/cm2

Figure 3: 500 mJ/cm^2 UVB produces mild edema

To test for onset and existence of edema, paw volume was monitored. Six separate groups (Control (0 mJ/cm^2) n=2, 60 mJ/cm^2 n=2; 150 mJ/cm^2; 350 mJ/cm2 n=7: 500 mJ/cm^2 n=5, CFA n=3). CFA produced significant swelling 2 hours after irradiation peaking at 48 hours with a mean volume of 2.4 ± 0.2 mL compared to control animals (1.5 ± 0.0 mL). Higher doses of UVB did produce increases in paw volume but not to the degree of CFA. 500 mJ/cm^2 produced an increase in paw volume 48 hours after irradiation (1.9 ± 0.1 mL) compared to controls at the same time (1.5 ± 0.0 mL). This subsided by 96 hours. 300 mJ/cm^2 UVB an increase in paw volume 72 hours after irradiation (1.9 ± 0.0 mL) compared controls (1.5 ± 0.0 mL) at this time.
Values expressed as mean volume ± sem. (2-way ANOVA with Bonferroni post-hoc test, $P > 0.05$) * 500 mJ/cm^2; # 300 mJ/cm^2

Figure 4

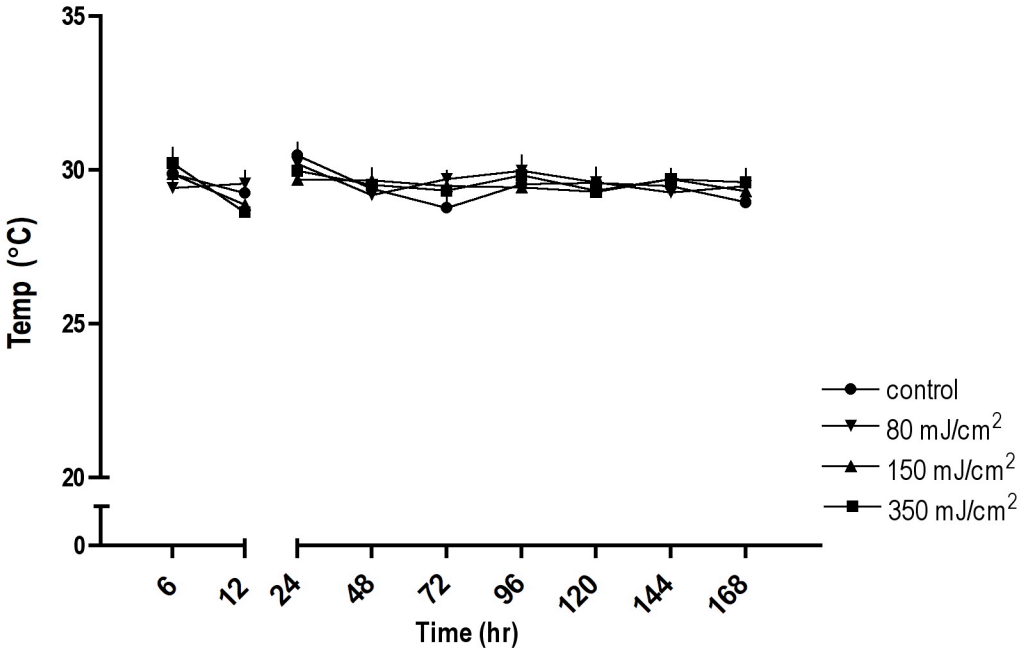
35
30
25
20
0
Temp (°C)
6
12
24
48
72
96
120
144
168
Time (hr)
control
80 mJ/cm2
150 mJ/cm2
350 mJ/cm2

Figure 4: UVB does not produce significant changes in cutaneous temperature

No significant change in paw temperature was observed following any dose of UVB. (2-way ANOVA compared to control).

Figure 5

Normal

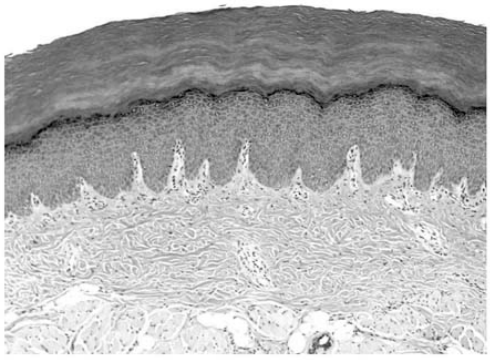

150 mJ/cm2

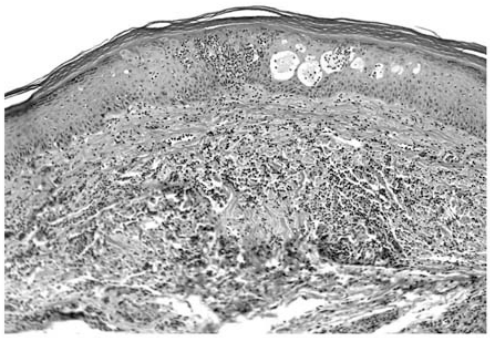

500 mJ/cm2

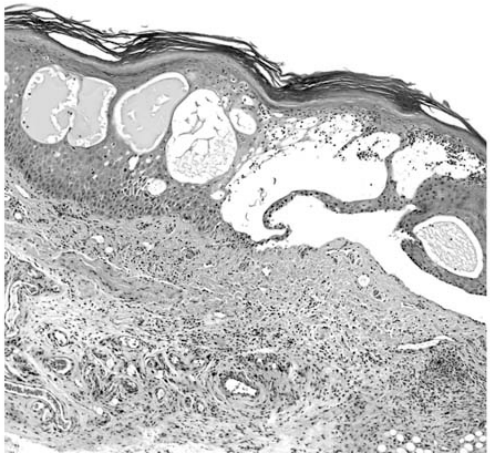

CFA

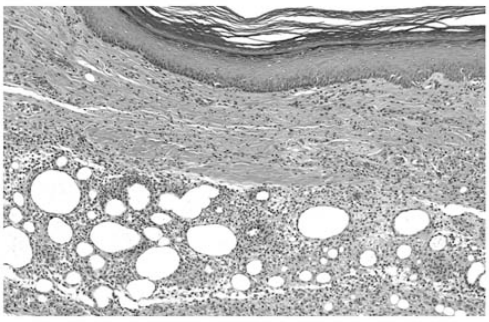

350 mJ/cm2

Summary:

Normal: no specific morphological findings

150 mJ/cm2: 96 hrs- mild intraepithelial vesicles, presence of neutrophils and mononuclear cells in dermis

350 mJ/cm2: 96 hrs- severe epidermal separation, prominent subepidermal separation, neutrophil and mononuclear cell infiltration in epeidermis, dermal edema

500 mJ.cm2: 48 hrs- severe epidermal separation, prominent subepidermal vesicle formation, neutrophil and mononuclear cell infiltrations in epidermis, dermal edema, spongiosis

CFA: 48 hrs- severe inflammation involving dermis characterized by neurtophils and poorly organized granulomatous inflamamtion

Figure 5: UVB and CFA produce severe inflammation but with differing characteristics

Above are representative examples of H & E slides taken from animals receiving a subcutaneous injection of CFA (48 hrs) or irradiated with 0 (96 hrs), 150 (96 hrs), 350 (96 hrs), or 500 mJ/cm^2 UVB (48 hrs). The 150 mJ/cm^2 dose clearly shows intraepithelial vesicle formation and dermal immune cell infiltration. Severe epithelial separation is apparent in epidermis exposed to 350 and 500 mJ/cm^2 doses of UVB. Epidermal infiltration of neutrophil and mononuclear cells is clearly evident as well. CFA had little effect of the epidermis but produced severe dermal edema and granulomatous inflammation.

Figure 6

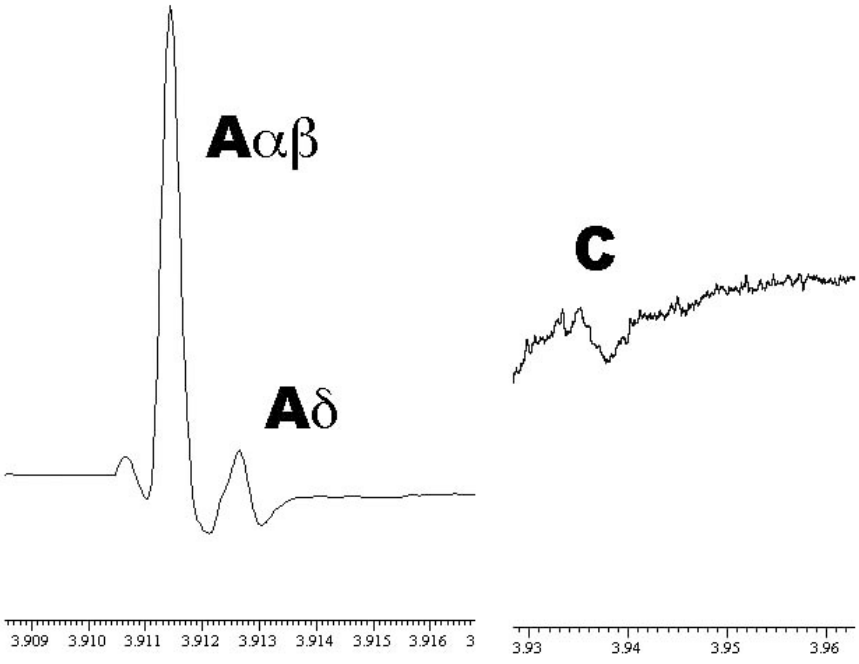
Aαβ
Aδ
C
3.909 3.910 3.911 3.912 3.913 3.914 3.915 3.916 3
3.93 3.94 3.95 3.96

Figure 6: Classification of single units by conduction velocity

This is a representative example of a compound action recording. There was no difference between compound action potential recordings taken from healthy skin and UVB irradiated skin so the data was combined. The mean conduction velocity range of the Aαβ waveform was 60.2 ± 12.3 m/s and16.6 ± 2.9 m/s with a mean of 27.9 ± 4.4 m/s. The Aδ waveform had a mean conduction velocity of 11.9 ± 2.8 m/s with an average range of 7.60 ± 1.9 m/s and 16.5 ± 4.1 m/s. The C waveform had a mean conduction velocity of 0.84 ± 0.2 m/s with a mean range of 1.09 ± 0.2 m/s and 0.59 ± 0.1 m/s. Units that had conduction velocities between the Aδ and C waves (4.0 and 1.5 m/s) were assigned to a C/Aδ group. All values expressed as mean ± sem.

Figure 7

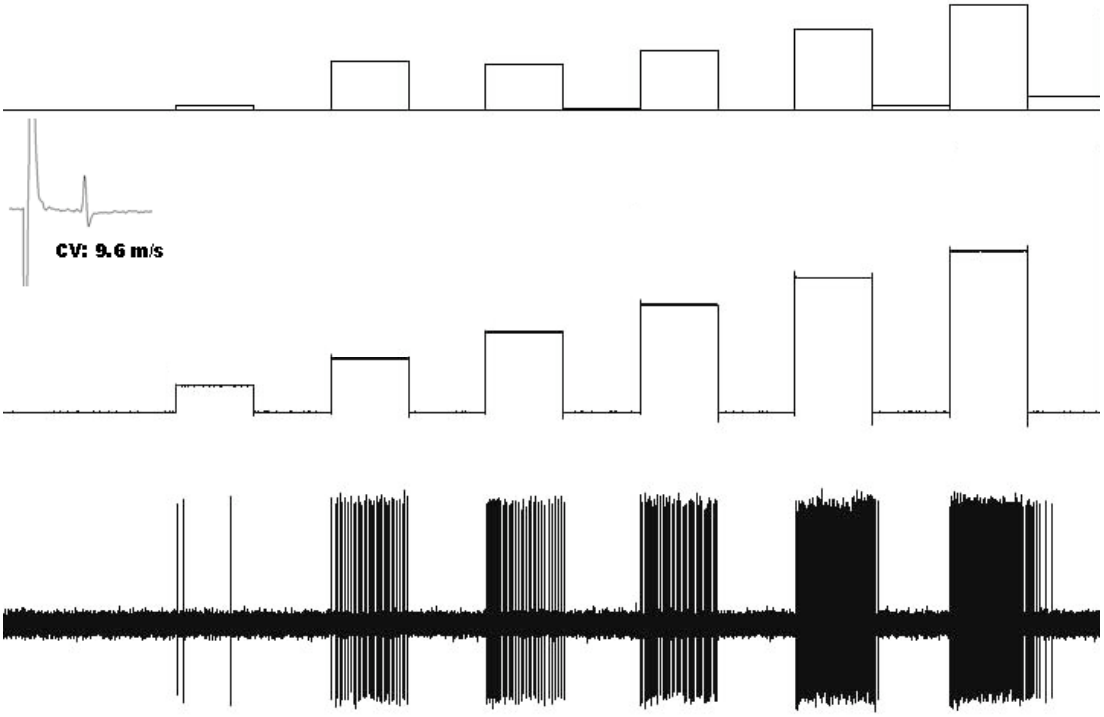

Figure 7: Graded mechanical stimulation

This is a representative example of graded mechanical stimulation to the cutaneous receptive field of a single Aδ-fiber using a computer controlled probe. The bottom shows the recorded action potentials, the middle depicts the increasing force delivered by a probe and the top shows a histogram of spikes per force (5secs). A unit was classified based on its stimulus-response relationship. A nociceptor was defined as a unit whose firing rate increased monotonically with increasing pressure of stimulation.

Figure 8

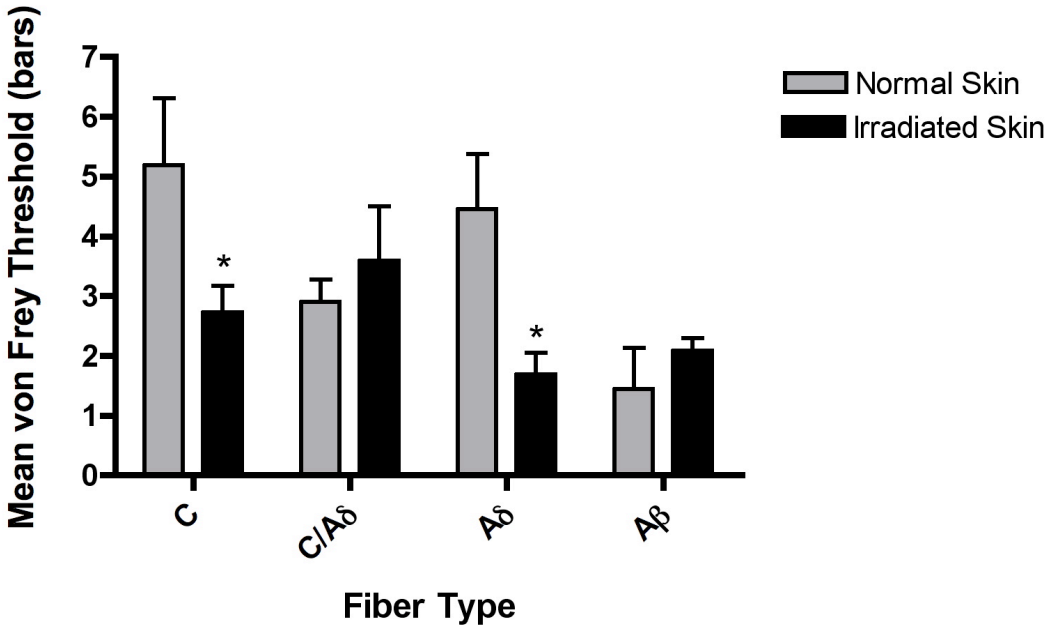
Mean von Frey Threshold (bars)
7
6
5
4
3
2
1
0
*
*
C
C/Aδ
Aδ
Aβ
Fiber Type
Normal Skin
Irradiated Skin

Figure 8: Mechanically thresholds of units innervating irradiated and inflamed skin

The mechanical thresholds of 46 units (25 from normal skin, 21 from irradiated skin) were measure using von Frey filaments. The mean von Frey threshold was significantly lower for C-fiber units (2.7 ± 0.4 bars) and Aδ units (1.7 ± 0.4 bars) innervating irradiated skin compared to C and Aδ innervating normal skin (5.2 ± 1.1 and 4.5 ± 0.9 bars respectively). Normal skin: C (n=7), C/Aδ (n=9), Aδ (n=7), Aβ (n=2); Irradiated skin: C (n=7), C/Aδ (n=6), Aδ (n=4), Aβ (n=4)

t-test < *0.05*

Figure 9

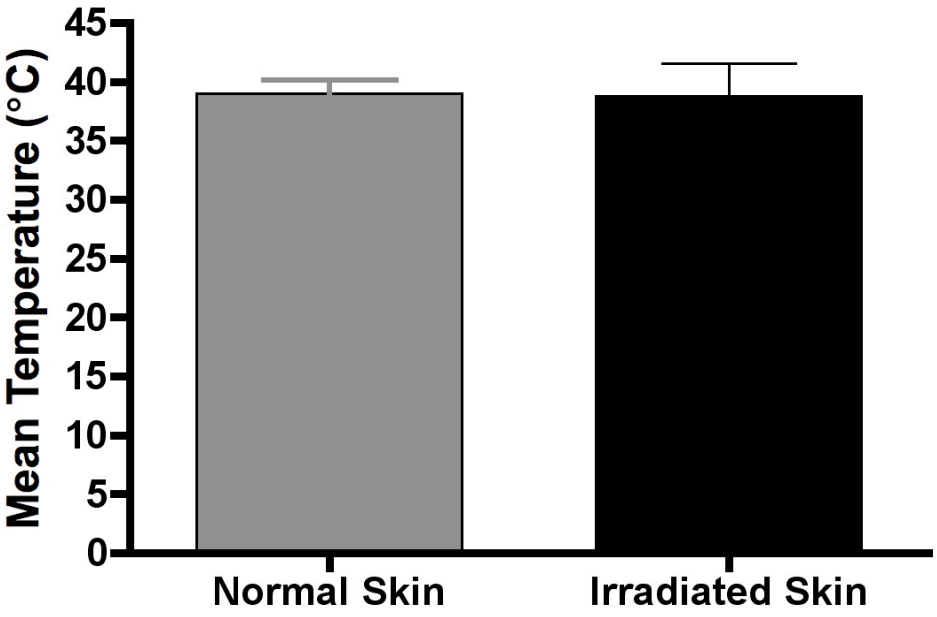
Mean Temperature (°C)
45
40
35
30
25
20
15
10
5
0
Normal Skin
Irradiated Skin

Figure 9: Heat thresholds for units innervating normal and irradiated skin

Heat thresholds for C-fiber units were not changed by UVB irradiation. Mean thresholds for C-fibers innervating normal skin (n=3) was 39.0 ± 1.2 ° compared to units innervating irradiated skin (n=4) 38.8 ± 2.8 °.

Chapter 4

Peripheral Actions of Morphine Sulfate on Nociceptor Activity in Irradiated Skin

Introduction

Changes in the excitability and sensitivity to chemical mediators occur in primary afferent fibers following injury or inflammation and are important mechanisms related to nociception and hyperalgesia. Data from chapter 2 demonstrated direct electrophysiological evidence for opioid modulation of primary afferent activity following CFA inflammation. These findings were consistent with previous work that demonstrated enhanced peripheral opioid receptor function following CFA inflammation (Wenk et al., 2006, Brederson and Honda, personal communication).

Evidence for UVB-induced inflammation has been described in the previous chapter including thermal hyperalgesia, mechanical allodynia and sensitization of primary afferent fibers. The release of pro-inflammatory mediators from primary afferent fibers, circulating leukocytes, and non-neuronal peripheral cells, occurs following UV irradiation (Saade et al., 2008; Legat et al., 2002; Eschenfelder et al., 1995; Hruza and Pentland, 1993). The release of these mediators is consistent with inflammation and lead to sensitization of primary afferent fibers (Dray and Bevan, 1993; Julius and Basbaum, 2001). In chapter 3, a dose of 350 mJ/cm^2 UVB increased spontaneous activity and reduced mechanical thresholds of nociceptors. This is consistent with increases in spontaneous firing (Andreev et al., 1994) and increases in baseline discharges (Eschenfelder et al., 1995; Szolcsanyi et al., 1987) of polymodal nociceptors exposed to broadband UV irradiation.

The aim of the present study is to examine the effect of morphine on nociceptors innervating UVB inflamed skin. Chapter 3 demonstrated that UVB produces severe inflammation but differs to that induced by CFA. Previous work and data from chapter 2 provides direct electrophysiological evidence for enhanced peripheral opioid receptor function following CFA inflammation (Wenk et al., 2006, Brederson and Honda, personal communication) but it is unknown whether UVB inflammation leads to changes in peripheral opioid receptor functioning. It has previously been demonstrated that peripherally applied morphine sulphate suppresses spontaneous activity of nociceptors following UV irradiation (Andreev et al., 1994) but it is unknown whether peripherally applied opiates modulate nociceptor response to mechanical stimuli. The present study, using an *in vitro* glabrous skin-nerve preparation will directly investigate whether morphine reduces mechanical response of nociceptors innervating UVB irradiated skin.

Methods

Preparation of Solutions

Synthetic interstitial fluid solution (SIF; on mM: 123 NaCl; 3.5 KCL, 0.7 MgSO4, 2.0 CaCl2, 9.5 Na gluconate, 1.7 NaH2PO4, 5.5 glucose, 7.5 sucrose, 10 HEPES; pH 7.45 ± 0.05) (Koltzenburg et al., 1997) was prepared the day of each experiment. Stock solution of morphine sulfate and naloxone

(Sigma; St. Louis, MO) were diluted with SIF (ph 7.45 ± 0.05). Both SIF and drug solutions were saturated before use.

Animals

All experimental procedures were approved by the Institutional Animal Care and Use Committee at the University of Minnesota and conform to established guidelines. A total of 22 adult male Sprague-Dawley rats, 250-300g were used in this study.

UVB irradiation

Rats were deeply anaesthetized with isofluorane and placed on their stomachs and shrouded with a UV opaque material with only the plantar surface of the right hind paw exposed, perpendicular to the narrowband UVB (Handisol, Amjo Corp, US) light source situated above. The narrowband UVB lamp emits a wavelength centered near 311nm. Irradiance produced by the bulbs during each session was determined at the distance of the limb from the light source using a calibrated meter UV340 Mannix UV light meter (General Tools & Instruments Company, NY, USA). A UVB dose of 350 mJ/cm^2 was used for all experiments. UVB dose was calculated using the following formula:

Dosage Energy = UV intensity (constant measured by UV light meter) x time.

Electrophysiology

Skin-Nerve Preparation

Rats were deeply anesthetized with a combination of ketamine, acepromazine and xylazine (6.8/0.09/0.45 mg/kg). The glabrous skin of the hindpaw was dissected and excised together with the attached tibial nerve and the medial and lateral branches of the plantar nerve. The skin was mounted corium side up in an organ bath and superfused with warmed (32°C) and oxygen-saturated SIF buffer. The nerves and tissue was cleaned of all muscle, tendons, and connective tissue. The cut end of the tibial nerve was threaded into a separate recording chamber and mounted on a dissecting mirror. Mineral oil was added to the chamber until the floating oil reached the level of the dissecting mirror. Nerve filaments were lifter into the mineral oil and placed on a gold recording electrode for extracellular recording. The reference electrode was placed in the recording chamber at the level of the buffer. Neural signals were amplified (DAM80, World Precision Instruments, Austin, TX), filtered, then displayed on two oscilloscopes and broadcast over an audio speaker. All data were collected using SPIKE 2 software (CED) and analyzed both on and off-line.

Compound Action Potential

At the beginning of most experiments, the medial or plantar nerve was stimulated electrically using an isolated monopolar electrode inserted through

the nerve. The entire cut end of the tibial nerve was place on the recording electrode and the stimulation intensity and duration of electrical stimulation were adjusted until Aβ, Aδ, and C fiber wave forms could clearly be viewed and recorded (compound action recordings for UVB irradiated skin were discussed in chapter 3). Distance between the two electrodes was measured by lying suture along the nerve branch using forceps. The conduction velocities obtained were used for the classification of single recorded units. Single units with conduction velocities that fell between the Aδ and C wave ranges were classified as C/Aδ units (Lawson and Waddell, 1990).

Single Unit Isolation and Receptive Field Localization

Using sharpened forceps, the nerve was repeatedly teased apart into smaller filaments unit single unit activity could be discriminated. The receptive field of an identified unit was first identified using a stimulating electrode. The stimulating electrode was placed at progressively distal sites along the nerve so the path of the axon could be determined. The stimulating electrode was positioned in the receptive field and an electrically evoked spike was recorded to determine the latency from the stimulus to the spike. Distance was measured using thin suture placed along nerve. Conduction velocity was expressed as meters per second**.** Mechanical stimulation was then applied using a fine smooth glass rod to the electrically identified receptive field to delineate receptive field boundaries. All units tested in the present study were mechanically sensitive.

Characterization of Mechanical Response Properties

Mechanical response properties were determined using a combination of two methods. First, mechanical threshold was determined using calibrated von Frey filaments applied to the corium surface in order of increasing pressure. Filaments ranged from 0.7 mN to 78.37 mN. Threshold was defined as the lowest force capable of evoking at least two impulses.

Stimulus-response relationships were then determined for each unit. Responses were measured a computer controlled mechanical probe (Aurora Scientific Inc. Ontario, Canada) which a diameter of 1.2mm that produced a graded mechanical stimuli (0.5–5.0 bars) for a duration of five seconds each. Nociceptors were defined as units whose firing rate increased monotonically with increasing pressure of stimulation. High threshold units that responded only to the maximal stimulus were also defined as nociceptors. The lowest force required to produce at least two impulses was reported as each unit's mechanical threshold. Each probe was positioned with a micromanipulator and lowered onto the receptive field. The stimulation onset and offset times were signaled to the online data acquisition program.

Spontaneous Activity

Unevoked baseline activity was recorded for at least 15 seconds before mechanical stimulation of the receptive field of each unit. Single units

that had unevoked baseline activity greater that 0.1 spikes/second were classified as spontaneously active.

Peripheral Morphine Testing

The conduction velocity, mechanical threshold, response to graded mechanical stimuli, and spontaneous activity were all determined for each unit before any drug testing took place. Drugs were applied directly to the corium surface of the skin through a small plastic ring that was sealed over the cutaneous receptive field with vacuum grease to create a separate reservoir.

The computer controlled mechanical probe delivered a suprathreshold (as determined using the graded mechanical stimulation paradigm) stimulation to the corium surface of the receptive field repeatedly for 5 seconds in 2-minute intervals. At least three stimulations were recorded before any drug testing to produce baseline level of mechanical stimulation. The drug reservoir was then emptied of SIF with a suction pipette and filled with oxygenated morphine sulfate, naloxone, or a combination of morphine sulfate and naloxone. Drug was allowed to remain for 2 minutes and then removed and the receptive field was repeatedly washed with SIF. Mechanical responses continued to be tested in 2 minute intervals until washout (at least 50% reversal of drug-induced response change).

Results

Distribution of Single Units

Data in this chapter are reported as the mean ± standard deviation.

A compound action potential was recorded at the beginning of most experiments (Figure 1). Single units were classified into fiber type (Aαβ, Aδ, or C) according to their conduction velocity and the waveform ranges recorded for each preparation's compound action recording. The mean conduction velocity for the Aαβ waveform was 27 ± 6.1 m/s with a range of 18.2 ± 4.8 m/s and 56 ± 14.5 m/s. The mean conduction velocity for the Aδ waveform was 9.65 ± 3.2 m/s with a range of 6.1 ± 1.8 and 14.7 ± 5.8 m/s. The C wave ranged from 0.59 ± 0.18 and 1.1 ± 0.21 m/s with a mean velocity of 0.85 ± 0.14 m/s.

The Aδ and C wave components of the action potentials never overlapped. The minimum conduction velocity recorded for the Aδ wave was 3.6 m/s, while the fastest conduction velocity measured for the C wave was 1.3.

Based on the above compound action potential recordings, single units with conduction velocities greater than 15 m/s were classified as Aαβ fibers. Units that conducted within 15 m/s and 4 m/s were classified as Aδ and all units conducting below 1 m/s was classified as C fibers. Units with

conduction velocities that fell between the Aδ and C range (conducting between 1 m/s and 4 m/s) were assigned to a C/Aδ category.

Classification of Identified Primary Afferent Units

A total of 18 units were isolated from tibial nerves of thirteen rats (Table 1). Of the units studied, 14 units were from UVB irradiated skin and 4 units were from normal healthy skin. Five of these units conducted within the Aδ range, 6 units had conduction velocities within the C/Aδ range, and 11 units conducted within the C range. No fibers used in this study had conduction velocities in the Aαβ range.

A stimulus-response measurement was recorded using a computer controlled mechanical probe that produced a graded mechanical pressure to the receptive field of each unit (Figure 2). Nociceptors have firing rates that increase monotonically with increasing pressure of stimulation. For the present study nociceptors were preferentially sought out and therefore all units were classified as nociceptors

<u>Aδ fiber Units</u>

A total of five units (2 normal skin, 3 irradiated skin) were classified as Aδ fibers. Fibers innervating irradiated skin had a mean conduction velocity of 8.1 ± 3.0 m/s and fibers innervating normal skin had a mean conduction velocity of 10.6 ± 2.2 m/s.

C/Aδ fiber Units

A total of 4 units (1 normal skin, 3 irradiated skin) were classified as C/Aδ fibers. Fibers innervating irradiated skin had a mean conduction velocity of 2.8 ± 0.4 m/s and the one unit tested innervating normal skin had a conduction velocity of 2.5 m/s.

C fiber Units

A total of 9 units (1 normal, 1 irradiated) were classified as C-fiber units. Units innervating irradiated skin had a mean conduction velocity of 0.9 ± 0.2 m/s and the one C-fiber tested that innervated normal skin had a conduction velocity of 0.68 m/s.

Response Variability and Criteria for Drug Effect

Reproducibility of single unit responses to repeated mechanical stimulation was assessed for each unit using a computer controlled mechanical probe. At least three mechanical stimulations were recorded before any drug testing to measure baseline (BL) responses (in spikes). The ratio of spikes between BL 1 and BL 2 was measured and the ratio of spikes between BL 2 and BL 3. The average BL ratio was then measured. The responses of units innervating inflamed and healthy skin did not differ and their responses were combined. The average BL spike ratio of all units was 1.05 ± 0.1.

Criteria had to be established in order to determine whether a change in response level after drug application was due to the action of the drug or was due to normal response variability. Following drug application two responses to mechanical stimulation were recorded and the average response was calculated. A positive drug effect was classified as a response that fell outside 2 standard deviations from the mean BL. To clarify, a unit was determined to be within normal variability if the mean response to mechanical stimulation after drug fell within 80 and 120% of the mean BL. A unit had a positive effect if the response after drug was above 120% or below 80% of the mean baseline response.

Morphine Sensitive Units

A total of 18 units (4 in normal skin, 14 in inflamed skin) were tested with 500 nM morphine sulphate. The concentration of 500 nM was selected based on concentration-response curves from earlier units innervating CFA inflamed skin. For a unit to be determined to be morphine sensitive, the unit's responses to mechanical stimulation after drug must meet the above criteria followed by a washout period where the response returns to a least 50% of BL.

Morphine significantly reduced mechanical responsiveness. As a population, morphine reduced mechanical responses to 72.5 ± 8.1% of BL compared to vehicle (97.2 ± 2.6%) (Figure 3).

Of the 14 units innervating UVB irradiated skin, the responses to mechanical stimulation of 8 units were reduced sufficiently to satisfy criteria for a positive morphine response. Of the units, 4 were classified as C fibers, 1 as an Aδ fiber, and 3 as C/ Aδ fibers. Additionally, 1 unit with a conduction velocity in the C range had an increased response (122.3% of BL) following morphine application. This unit was included in the population data but was not included when positive drug effects were examined. Of the 8 units that were classified as morphine sensitive, 4 were spontaneously active. Three of these units also showed reduction in spontaneous activity after morphine application. The mean percent baseline response of units that met the criteria of a drug responder was 51.6 ± 7.4% (Figure 4).

Morphine did not change mechanical responsiveness in any of the 4 units innervating normal healthy skin that were examined. The mean percent of baseline response was 95.5 ± 7.4% (Figure 4).

Units Treated With Naloxone Only Or Naloxone + Morphine Sulphate

Three morphine sensitive units were treated with 500 nM morphine sulphate + 1 μM Naloxone after a significant washout period. Of the 3 units, 1 was classified as a C fiber and the other 2 were C/Aδ units. In all 3 cases, morphine did not have a significant effect on mechanical responses when treated along with the antagonist naloxone (Figure 3). This indicates that the opioid receptor antagonist blocked the effect of morphine suggesting a receptor mediated event.

Three fibers innervating irradiated skin were treated with 1 μM naloxone only. One unit was classified as C/Aδ units and 2 units had conduction velocities in the C range. Mean percent of baseline response was 104.2 ± 7.0% indicating that the antagonist alone did not have an effect on mechanical responses (Figure 3).

Discussion

The purpose of the present experiments was to examine whether UVB irradiation leads to the activation of the endogenous peripheral opioid analgesic system using a rat *in vitro* glabrous skin-nerve preparation. The mechanical response properties of 18 primary afferent single units (4 from normal healthy skin and 14 from irradiated skin) were measured. As a population, morphine reduced the mechanical responses of 57% of all units treated. Morphine sensitive fibers showed a 49% decrease in response to mechanical stimuli following drug application. The inhibitory effect was blocked by the nonselective opioid receptor antagonist naloxone. These findings are consistent with previous reported data from our lab that demonstrated activation of the peripheral opioid analgesic system 28 hours following CFA-induced inflammation (Wenk et al., 2006). Data reported in Chapter 2 show that this analgesic system is still functional 72 following CFA-induced inflammation. In all experiments, morphine did not alter the responses of nociceptors innervating normal skin consistent with the idea that peripheral opioid analgesia is enhanced following inflammation and/or

damage. Underlying mechanisms following both types of inflammation may directly change the functional competence of opioid receptors located on peripheral nerves and terminals or lead to changes in the surrounding environment that indirectly lead to such changes.

Additionally, morphine suppressed spontaneous activity of 3 of the 8 morphine sensitive units. This is consistent with previous research that demonstrated that morphine suppresses spontaneous activity of nociceptors following broadband UV irradiation (Andreev et al., 1994). This data is further evidence that UVB induced inflammation leads to enhanced peripheral opioid receptor function.

It is likely that pro-inflammatory mediators released following UV irradiation leads to inflammation and sensitization of primary afferent fibers. NGF and Il-1 levels are increased following UV irradiation at times consistent with behavioral changes observed in chapter 3 (Saade et al. 2008). UV also leads to the increases in histamine, substance P and CGRP release (Legat et al., 2002; Eschenfelder et al., 1995; Hruza and Pentland, 1993) and increased levels of arachidonic acid and prostaglandins (Black et al., 1980; Gilchrest et al., 1981).

Though UVB induced inflammation differs from CFA induced inflammation, similar mechanisms may underlie enhanced peripheral opioid receptor function. Cytokines, like Il-1, can lead to release of endogenous opioid ligands from circulating leukocytes (Schäfer et al., 1994; Cabot et al., 1997, 2001; Binder et al., 2004). The presence of ligand can mediate

translocation of opioid receptors from internal stores to the plasma membrane (Coggeshall et al., 1997) increasing receptor availability. Furthermore, many proinflammatory mediators can regulate changes in opioid receptor function through receptor interactions. Bradykinin is released during inflammation. Activation of can induce membrane insertion of intracellular DOR and induce functional competence (Patwardhan et al., 2005) through it interaction with the B2 bradykinin receptor located on primary afferent fibers. Chemokines may also modulate opioid receptor function through coupling (Parenty et al., 2008.

In summary, morphine reduced the mechanical responses of 57% of the units innervating UVB irradiated skin but did not have a significant effect of mechanical response of nociceptors innervating normal skin. This inhibitory effect was blocked by the nonselective opioid receptor antagonist naloxone. This data provides direct electrophysiological evidence for functional peripheral opioid receptors following UVB irradiation

Table 1

	NORMAL SKIN	IRRADIATED SKIN (350 MJ/CM^2)
Aδ	N=2 Mean CV: 10.6 ± 2.2 m/s Spontaneous: 1 of 2 (50%)	N=3 Mean CV: 8.1 ± 3.0 m/s Spontaneous: 1 of 3 (33%)
C/Aδ	N=1 CV: 2.5 m/s Spontaneous: 0%	N=3 Mean CV: 2.8 ± 0.4 Spontaneous: 1 of 3 (33%)
C	N=1 CV: 0.68 m/s Spontaneous: 0%	N=8 Mean CV: 0.9 ± 0.2 m/s Spontaneous: 6 of 8 (75%)

Figure 1

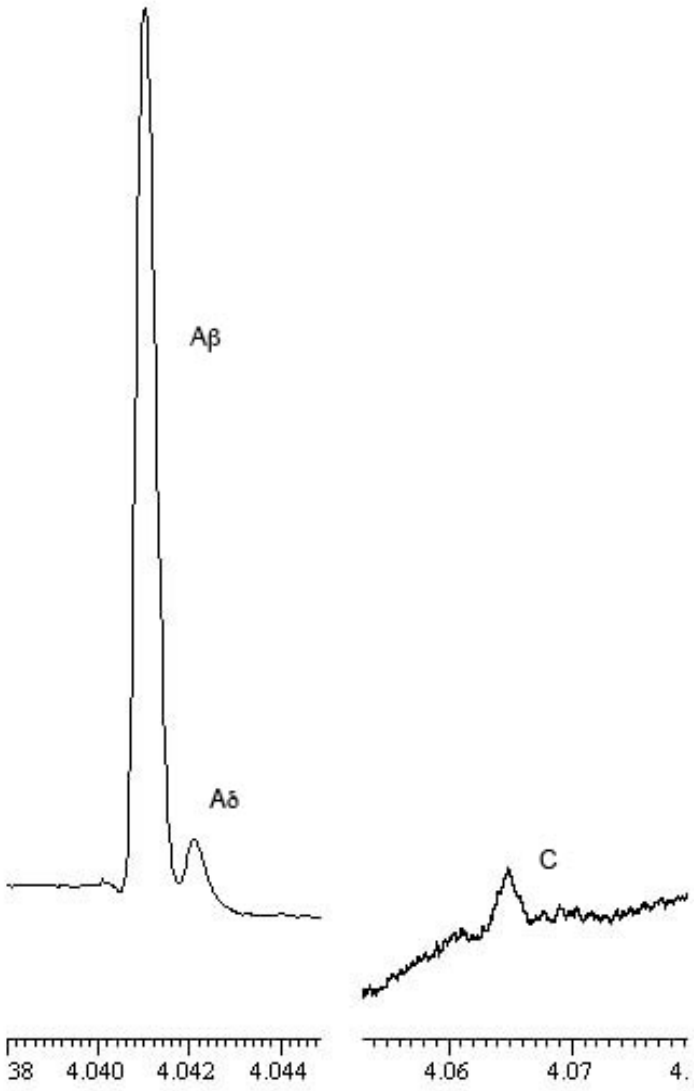

Figure 1: Classification of single units by conduction velocity

This is a representative example of a compound action potential recording. Single units were classified into fiber type (Aαβ, Aδ, or C) according to their conduction velocity. The mean conduction velocity for the Aαβ waveform was 27 ± 6.1 m/s with a range of 18.2 ± 4.8 m/s and 56 ± 14.5 m/s. The mean conduction velocity for the Aδ waveform was 9.65 ± 3.2 m/s with a range of 6.1 ± 1.8 and 14.7 ± 5.8 m/s. The C wave ranged from 0.59 ± 0.18 and 1.1 ± 0.21 m/s with a mean velocity of 0.85 ± 0.14 m/s. Units with conduction velocities between1 m/s and 4 m/s were assigned to a C/Aδ category

Figure 2

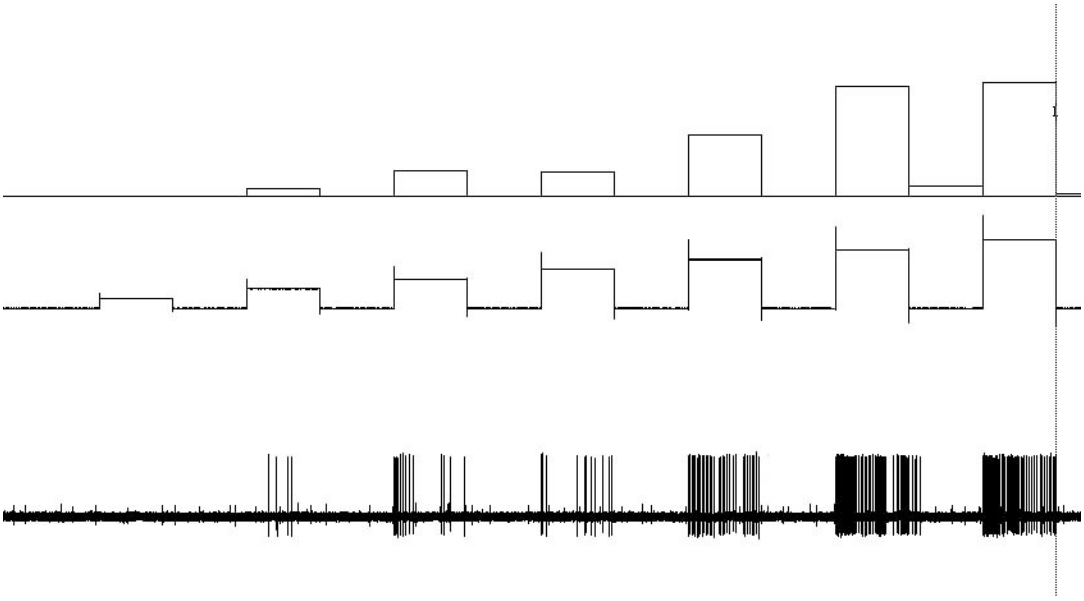

Figure 2: Graded mechanical stimulation

This is a representative example of graded mechanical stimulation to the cutaneous receptive field of a single primary afferent fiber. The bottom trace depicts the recorded action potentials. The middle trace is a representation of the increasing force (0.5 – 3.5 bars) delivered by a probe with a histogram of spikes per force (5secs) at the top. A unit was classified based on its stimulus-response relationship. A nociceptor was defined as a unit whose firing rate increased monotonically with increasing pressure of stimulation

Figure 3

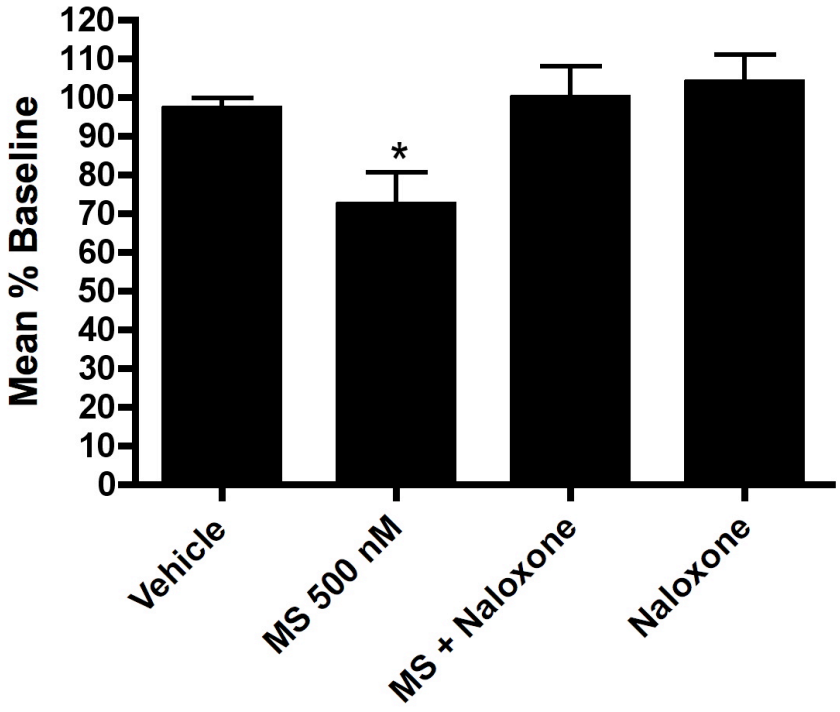
Mean % Baseline
120
110
100
90
80
70
60
50
40
30
20
10
0
*
Vehicle
MS 500 nM
MS + Naloxone
Naloxone

Figure 3: Morphine inhibits mechanical responsiveness

As a population, morphine reduced primary afferent fiber response to mechanical stimulation. This effect was blocked by co-application of morphine and naloxone. To test for endogenous basil opioid activity, naloxone was applied to the receptive field of three units. No significant effect was observed. Vehicle (n=14) mean % response 97.2 ± 2.6; Morphine (n=14) mean % response 72.5 ± 8.1; MS + Naloxone (n=3) mean % response 100.4 ± 7.9; Naloxone (n=3) mean % response 104.2 ± 7.0. (one-way ANOVA, with Bonforoni post hoc tests, $P > 0.05$).

Figure 4

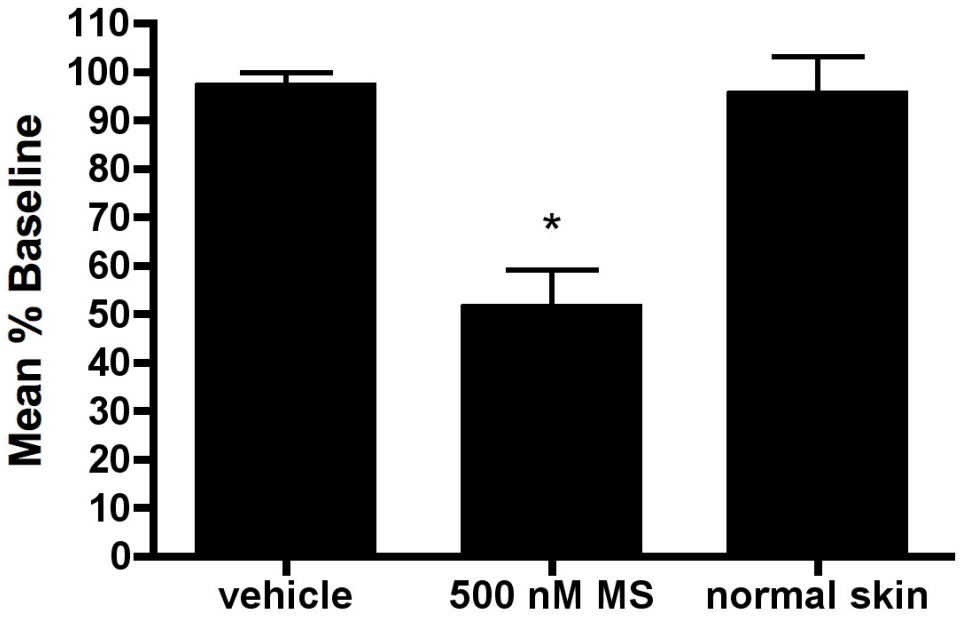
Mean % Baseline
110
100
90
80
70
60
50
40
30
20
10
0
*
vehicle
500 nM MS
normal skin

Figure 4: Morphine reduces mechanical responsiveness in irradiated skin but not normal skin

Eight of 14 (57%) units treated with morphine had reduced mechanical responses following drug application (mean percent baseline 51.6 ± 7.4%). Of the 8 units that were classified as morphine sensitive, 4 were spontaneously active. Three of these units also showed reduction in spontaneous activity after morphine application. Morphine did not change mechanical responsiveness of units innervating normal skin (n=4; mean % baseline 95,5 ± 7.4%). This data is consistent with previous research that demonstrates increased opioid receptor efficacy following inflammation. (one-way ANOVA, with Bonforoni post hoc tests, $P > 0.05$).

Chapter 5

Conclusion and Discussion

The purpose of this thesis was two-fold. The first aim was to determine whether mu opioid receptors (MOR) on primary afferent fibers are differentially regulated during early and late phases of CFA Inflammation. The second aim was to characterize a new model of UVB inflammation and determine whether UVB inflammation leads to sensitization of primary afferent fibers and leads to the activation of a peripheral opioid analgesic system.

Effects of Morphine on Single Unit Responses in CFA Inflamed Skin

The data presented in chapter two provide evidence that MOR is differentially regulated during early and late stages of inflammation. Earlier work from our lab as shown that morphine reduces the responses of C-fiber nociceptors to both thermal and mechanical stimuli during early inflammation (18 hour) (Wenk et al., 2006). At the concentrations tested, it was unknown what opioid receptor, or combination of receptors, produced the effects observed following morphine application to the receptive field of isolated primary afferent fibers. In the first studies to directly test selective opioid receptor agonists using the glabrous *in vivo* skin-nerve preparation, our lab has shown that the activation of DOR, by the DOR selective agonist deltorphin II, reduced the mechanical responsiveness of C-fiber nociceptors innervating 18 hour CFA inflamed skin (Brederson and Honda, personal communication). The percent of fibers that were deltorphin II-sensitive were

similar to what we previously found when fibers innervating 18-hour inflamed skin were treated with morphine. These findings indicate the DOR is functional 18 hours following CFA inflammation and may underlie the effects observed following morphine administration.

To determine whether MOR is functional following CFA-induced inflammation and contributes to attenuation of mechanical responses following morphine application to the receptive field of sensitized primary afferent fibers, the MOR selective agonist DAMGO was directly applied to the cutaneous receptive field of identified nociceptors innervating 18 hour inflamed skin. DAMGO did not significantly alter nociceptive responses to mechanical stimulation. Taken together with previous research from our lab, this data suggests that DOR is mainly responsible for morphine's effects on the mechanical responses of nociceptors in 18 hour inflamed skin. The effects of DOR or MOR selective agonists on thermal response properties have not been studied so it is unknown whether MOR is functional on a sub-population of nociceptors dedicated to thermal responses.

CFA leads an increase in MOR synthesis and trafficking (Hassan et al., 1993; Shaqura et al., 2004). It is unlikely that MOR could be synthesized and trafficked to the periphery by 18 hours, but up-regulation of the receptor could account for any changes seen at a later stage (72 hours) of inflammation (Stein et al., 1990). CFA produces severe inflammation as early as hours and continues for days. This inflammation could also produce changes in the environment that could alter receptor function. Consistent with this are the

findings that bradykinin and chemokines, both of which are released during inflammation, have regulatory effects on opioid receptors (Patwardhan et al., 2005; Parenty et al., 2008).

We examined whether morphine sulphate and DAMGO attenuate the mechanical responses of nociceptive units innervating 72 hour inflamed skin. Morphine had similar effects in 72 hour inflamed skin as it did in 18 hour inflamed skin. DAMGO did not alter response properties of nociceptive fibers in 18 hour inflamed skin but produced significant reductions to the mechanical response properties of nociceptive fibers innervating 72 our inflamed skin suggesting increased MOR efficacy. DAMGO effects were concentration dependent and antagonist reversible, indicating that they were receptor mediated.

Characterization of a UVB Model of Inflammation

The data presented in chapter three further characterizes a model of hyperalgesia produced by a single exposure of the glabrous skin of the rat's hind limb to UVB light. It also demonstrates that UVB produces significant inflammation that differs that produced by CFA.

We first looked at the classical signs of inflammation: pain, heat and edema. UVB produced dose-dependent mechanical allodynia as well as thermal hyperalgesia comparable to the commonly used CFA model of inflammation. Higher doses of UVB produced significant swelling though not

to the extent produced by CFA, no significant changes in cutaneous temperature were observed.

Taken together, UVB produces many of the classical signs of inflammation. To further characterize this we first looked at pathological changes in skin after CFA or UVB irradiation. Histopathological analysis revealed major differences in the UV- and CFA-induced tissue responses. The response to CFA predominantly involved the dermis with acute inflammation observed as early as 4 hours progressing to poorly organized granulomatous inflammation at 48 hours and sustained granulomatous response by 168 hours. UV damage was not observed at 4 hours but was prominent at 48 hours. The UV-induced lesions predominantly involved the epidermis, in contrast to CFA that was associated with a dermal response. There also was early resolution of the UV-induced injury present at the 96 hours with almost complete resolution at 168 hours. These findings are consistent with a single, transient, but severe and dose-dependent injury induced by UV, in contrast to chronic, sustained injury caused by CFA.

Next, using an *in vivo* skin nerve preparation, we examined whether UVB irradiation resulted in the sensitization of primary afferent fibers. Initial findings suggest that UVB results in an increase in spontaneous activity of primary afferent fibers innervating irradiated skin and leads to a decrease in mechanical thresholds. These findings indicate that UVB does lead to sensitization of primary afferent fibers.

Effect of Morphine Sulphate on Single Units Innervating Irradiated Skin

Chapter three provided evidence that UVB causes inflammation, resulting in hyperalgesia, edema, and sensitization of primary afferent fibers. There is also evidence that the inflammation differs from that caused by CFA. Earlier work from our lab and data from chapter two provide direct electrophysiological evidence that CFA inflammation enhances opioid receptor functioning. In chapter four, I tested the effects of morphine sulphate on nociceptors innervating UVB irradiated skin in order to determine whether opioid receptor efficacy is enhanced under the type of inflammation produced by UVB. Morphine sulphate produced a concentration dependent and antagonist reversible reduction of mechanical responses in nociceptors innervating irradiated skin indicating the effect was receptor mediated.

Discussion

Data presented in this thesis adds to the burgeoning evidence for an endogenous peripheral opioid analgesic system that is enhanced under inflammatory conditions. It is also becoming increasingly clear that this system is dynamic and the functional state of individual opioid receptors is a complex process that involves interactions with various peripheral systems (nervous, immune, endocrine, cutaneous). Interactions between these systems lead to a variety of functional states for opioid receptors that underlie the varying actions of opioid receptors (tolerance, sensitization, desensitization and dimerization). Further investigation into the molecular

mechanisms underlying these interactions is necessary and will lead to increased understanding of opioid receptor function. Understanding state-dependent changes of opioid receptor function will lead to enhanced and selective therapeutic strategies with less of the detrimental side effects.

Data presented also contribute to the characteristic of a new UVB-induced model of inflammation. UVB irradiation leads to pronounced inflammation leading to hyperalgesia, edema, and activation of immune responses. This model is a useful model for the study of hyperalgesia. UVB-induced inflammation is straightforward and quickly and accurately leads to pronounced hyperalgesia. This model differs from other currently used animal models of hyperalgesia in that it can be easily translated to human studies. But like other inflammatory models, UVB leads to enhanced function of the endogenous peripheral opioid system. Further studies that look at the molecular similarities and differences of these two inflammatory models are needed in order to understand the pathways that may lead to changes in the functional state of opioid receptors. Specific experiments that are needed include examination of the proinflammatory mediators that are released following inflammation in areas surrounding peripheral opioid receptors. Furthermore, changes in opioid receptor access may be very important in enhancing opioid therapies. Experiments that analyze the perineurium breakdown observed following inflammatory states and changes in receptor upregulation and trafficking may lead strategies that may be able to use the

body's own mechanisms to enhance the efficacy of already available pharmaceutics.

Many cells in the peripheral nervous system produce opioid compounds including keratinocytes, immune cells, and sensory neurons. These opioids are packaged and release in a Ca^{2+} dependent manner following receptor binding of various endogenous compounds including Il-1, CRF, cannabinoids and endothelin. It may be possible in the future to exploit these systems into producing opioids and releasing them in specific areas to produce localized opioid analgesia.

Further examination of peripheral opioid analgesic systems may provide new therapeutic tools for the treatment of pain while reducing side effects that impede the use of narcotics. Investigation into the relationship between inflammation and hyperalgesia may lead to a better understanding of the mechanisms underlying hyperalgesia leading to the discovery of new therapeutic targets and the development of new and superior treatments.

Bibliography

Acosta, C.G. and Lopez, H.S., delta opioid receptor modulation of several voltage-dependent Ca(2+) currents in rat sensory neurons, J Neurosci, 19 (1999) 8337-48.

Andreev, N., Urban, L. and Dray, A., Opioids suppress spontaneous activity of polymodal nociceptors in rat paw skin induced by ultraviolet irradiation, Neuroscience, 58 (1994) 793-8.

Antonijevic, I., Mousa, S.A., Schafer, M. and Stein, C., Perineurial defect and peripheral opioid analgesia in inflammation, J Neurosci, 15 (1995) 165-72.

Arvidsson, U., Riedl, M., Chakrabarti, S., Lee, J.H., Nakano, A.H., Dado, R.J., Loh, H.H., Law, P.Y., Wessendorf, M.W. and Elde, R., Distribution and targeting of a mu-opioid receptor (MOR1) in brain and spinal cord, J Neurosci, 15 (1995) 3328-41.

Barbacid, M., Structural and functional properties of the TRK family of neurotrophin receptors, Ann N Y Acad Sci, 766 (1995) 442-58.

Beckett, A.H. and Casy, A.F., Stereochemistry of certain analgesics, Nature, 173 (1954) 1231-2.

Beltramo, M., Bernardini, N., Bertorelli, R., Campanella, M., Nicolussi, E., Fredduzzi, S. and Reggiani, A., CB2 receptor-mediated antihyperalgesia: possible direct involvement of neural mechanisms, Eur J Neurosci, 23 (2006) 1530-8.

Besse, D., Lombard, M.C., Zajac, J.M., Roques, B.P. and Besson, J.M., Pre- and postsynaptic distribution of mu, delta and kappa opioid receptors in the superficial layers of the cervical dorsal horn of the rat spinal cord, Brain Res, 521 (1990) 15-22.

Bi, J., Tsai, N.P., Lin, Y.P., Loh, H.H. and Wei, L.N., Axonal mRNA transport and localized translational regulation of kappa-opioid receptor in primary neurons of dorsal root ganglia, Proc Natl Acad Sci U S A, 103 (2006) 19919-24.

Bigliardi, E., Bernuzzi, A.M., Corona, S., Gatti, S., Scaglia, M. and Sacchi, L., In vitro efficacy of nikkomycin Z against the human isolate of the

microsporidian species Encephalitozoon hellem, Antimicrob Agents Chemother, 44 (2000) 3012-6.

Binder, W., Mousa, S.A., Sitte, N., Kaiser, M., Stein, C. and Schafer, M., Sympathetic activation triggers endogenous opioid release and analgesia within peripheral inflamed tissue, Eur J Neurosci, 20 (2004) 92-100.

Bishop, T., Hewson, D.W., Yip, P.K., Fahey, M.S., Dawbarn, D., Young, A.R. and McMahon, S.B., Characterisation of ultraviolet-B-induced inflammation as a model of hyperalgesia in the rat, Pain, 131 (2007) 70-82.

Black, A.K., Fincham, N., Greaves, M.W. and Hensby, C.N., Time course changes in levels of arachidonic acid and prostaglandins D2, E2, F2 alpha in human skin following ultraviolet B irradiation, Br J Clin Pharmacol, 10 (1980) 453-7.

Brack, A., Rittner, H.L., Machelska, H., Shaqura, M., Mousa, S.A., Labuz, D., Zollner, C., Schafer, M. and Stein, C., Endogenous peripheral antinociception in early inflammation is not limited by the number of opioid-containing leukocytes but by opioid receptor expression, Pain, 108 (2004) 67-75.

Cabot, P.J., Carter, L., Gaiddon, C., Zhang, Q., Schafer, M., Loeffler, J.P. and Stein, C., Immune cell-derived beta-endorphin. Production, release, and control of inflammatory pain in rats, J Clin Invest, 100 (1997) 142-8.

Cabot, P.J., Carter, L., Schafer, M. and Stein, C., Methionine-enkephalin-and Dynorphin A-release from immune cells and control of inflammatory pain, Pain, 93 (2001) 207-12.

Cabral, G.A. and Staab, A., Effects on the immune system, Handb Exp Pharmacol (2005) 385-423.

Cahill, C.M., Morinville, A., Lee, M.C., Vincent, J.P., Collier, B. and Beaudet, A., Prolonged morphine treatment targets delta opioid receptors to neuronal plasma membranes and enhances delta-mediated antinociception, J Neurosci, 21 (2001) 7598-607.

Casanova, M.L., Blazquez, C., Martinez-Palacio, J., Villanueva, C., Fernandez-Acenero, M.J., Huffman, J.W., Jorcano, J.L. and Guzman, M., Inhibition of skin tumor growth and angiogenesis in vivo by activation of cannabinoid receptors, J Clin Invest, 111 (2003) 43-50.

Chaplan, S.R., Bach, F.W., Pogrel, J.W., Chung, J.M. and Yaksh, T.L., Quantitative assessment of tactile allodynia in the rat paw, J Neurosci Methods, 53 (1994) 55-63.

Chen, J.J., Dymshitz, J. and Vasko, M.R., Regulation of opioid receptors in rat sensory neurons in culture, Mol Pharmacol, 51 (1997) 666-73.

Coggeshall, R.E. and Carlton, S.M., Receptor localization in the mammalian dorsal horn and primary afferent neurons, Brain Res Brain Res Rev, 24 (1997) 28-66.

Czlonkowski, A., Stein, C. and Herz, A., Peripheral mechanisms of opioid antinociception in inflammation: involvement of cytokines, Eur J Pharmacol, 242 (1993) 229-35.

Dado, R.J., Law, P.Y., Loh, H.H. and Elde, R., Immunofluorescent identification of a delta (delta)-opioid receptor on primary afferent nerve terminals, Neuroreport, 5 (1993) 341-4.

Davies, S.L., Siau, C. and Bennett, G.J., Characterization of a model of cutaneous inflammatory pain produced by an ultraviolet irradiation-evoked sterile injury in the rat, J Neurosci Methods, 148 (2005) 161-6.

Dixon, W.J., Efficient analysis of experimental observations, Annu Rev Pharmacol Toxicol, 20 (1980) 441-62.

Dray, A. and Perkins, M., Bradykinin and inflammatory pain, Trends Neurosci, 16 (1993) 99-104.

Du, J., Koltzenburg, M. and Carlton, S.M., Glutamate-induced excitation and sensitization of nociceptors in rat glabrous skin, Pain, 89 (2001) 187-98.

Eschenfelder, C.C., Benrath, J., Zimmermann, M. and Gillardon, F., Involvement of substance P in ultraviolet irradiation-induced inflammation in rat skin, Eur J Neurosci, 7 (1995) 1520-6.

Ferreira, S.H. and Nakamura, M., III - Prostaglandin hyperalgesia: relevance of the peripheral effect for the analgesic action of opioid-antagonists, Prostaglandins, 18 (1979) 201-8.

Ferreira, S.H. and Nakamura, M., II - Prostaglandin hyperalgesia: the peripheral analgesic activity of morphine, enkephalins and opioid antagonists, Prostaglandins, 18 (1979) 191-200.

Ferreira, S.H. and Nakamura, M., I - Prostaglandin hyperalgesia, a cAMP/Ca2+ dependent process, Prostaglandins, 18 (1979) 179-90.

Gilchrest, B.A., Soter, N.A., Stoff, J.S. and Mihm, M.C., Jr., The human sunburn reaction: histologic and biochemical studies, J Am Acad Dermatol, 5 (1981) 411-22.

Goldstein, A., Tachibana, S., Lowney, L.I., Hunkapiller, M. and Hood, L., Dynorphin-(1-13), an extraordinarily potent opioid peptide, Proc Natl Acad Sci U S A, 76 (1979) 6666-70.

Griffin, G., Fernando, S.R., Ross, R.A., McKay, N.G., Ashford, M.L., Shire, D., Huffman, J.W., Yu, S., Lainton, J.A. and Pertwee, R.G., Evidence for the presence of CB2-like cannabinoid receptors on peripheral nerve terminals, Eur J Pharmacol, 339 (1997) 53-61.

Guindon, J. and Hohmann, A.G., Cannabinoid CB2 receptors: a therapeutic target for the treatment of inflammatory and neuropathic pain, Br J Pharmacol, 153 (2008) 319-34.

Hargreaves, K., Dubner, R., Brown, F., Flores, C. and Joris, J., A new and sensitive method for measuring thermal nociception in cutaneous hyperalgesia, Pain, 32 (1988) 77-88.

Harrison, G.I. and Young, A.R., Ultraviolet radiation-induced erythema in human skin, Methods, 28 (2002) 14-9.

Hassan, A.H., Ableitner, A., Stein, C. and Herz, A., Inflammation of the rat paw enhances axonal transport of opioid receptors in the sciatic nerve and increases their density in the inflamed tissue, Neuroscience, 55 (1993) 185-95.

Hoffmann, K., Kaspar, K., von Kobyletzki, G., Stucker, M. and Altmeyer, P., UV transmission and UV protection factor (UPF) measured on split skin following exposure to UVB radiation--correlation with the minimal erythema dose (MED), Photodermatol Photoimmunol Photomed, 15 (1999) 133-9.

Honda, C.N. and Arvidsson, U., Immunohistochemical localization of delta- and mu-opioid receptors in primate spinal cord, Neuroreport, 6 (1995) 1025-8.

Hruza, L.L. and Pentland, A.P., Mechanisms of UV-induced inflammation, J Invest Dermatol, 100 (1993) 35S-41S.

Hughes, J., Smith, T., Morgan, B. and Fothergill, L., Purification and properties of enkephalin - the possible endogenous ligand for the morphine receptor, Life Sci, 16 (1975) 1753-8.

Ibrahim, M.M., Porreca, F., Lai, J., Albrecht, P.J., Rice, F.L., Khodorova, A., Davar, G., Makriyannis, A., Vanderah, T.W., Mata, H.P. and Malan, T.P., Jr., CB2 cannabinoid receptor activation produces antinociception by stimulating peripheral release of endogenous opioids, Proc Natl Acad Sci U S A, 102 (2005) 3093-8.

Ji, R.R., Zhang, Q., Law, P.Y., Low, H.H., Elde, R. and Hokfelt, T., Expression of mu-, delta-, and kappa-opioid receptor-like immunoreactivities in rat dorsal root ganglia after carrageenan-induced inflammation, J Neurosci, 15 (1995) 8156-66.

Joris, J.L., Dubner, R. and Hargreaves, K.M., Opioid analgesia at peripheral sites: a target for opioids released during stress and inflammation?, Anesth Analg, 66 (1987) 1277-81.

Joris, J., Costello, A., Dubner, R. and Hargreaves, K.M., Opiates suppress carrageenan-induced edema and hyperthermia at doses that inhibit hyperalgesia, Pain, 43 (1990) 95-103.

Julius, D. and Basbaum, A.I., Molecular mechanisms of nociception, Nature, 413 (2001) 203-10.

Kauser, S., Schallreuter, K.U., Thody, A.J., Gummer, C. and Tobin, D.J., Regulation of human epidermal melanocyte biology by beta-endorphin, J Invest Dermatol, 120 (2003) 1073-80.

Koltzenburg, M., Stucky, C.L. and Lewin, G.R., Receptive properties of mouse sensory neurons innervating hairy skin, J Neurophysiol, 78 (1997) 1841-50.

Koppert, W., Brueckl, V., Weidner, C. and Schmelz, M., Mechanically induced axon reflex and hyperalgesia in human UV-B burn are reduced by systemic lidocaine, Eur J Pain, 8 (2004) 237-44.

Lamotte, C., Pert, C.B. and Snyder, S.H., Opiate receptor binding in primate spinal cord: distribution and changes after dorsal root section, Brain Res, 112 (1976) 407-12.

Law, P.Y. and Loh, H.H., Regulation of opioid receptor activities, J Pharmacol Exp Ther, 289 (1999) 607-24.

Legat, F.J., Griesbacher, T., Schicho, R., Althuber, P., Schuligoi, R., Kerl, H. and Wolf, P., Repeated subinflammatory ultraviolet B irradiation increases substance P and calcitonin gene-related peptide content and augments

mustard oil-induced neurogenic inflammation in the skin of rats, Neurosci Lett, 329 (2002) 309-13.

Li, C.H. and Chung, D., Primary structure of human beta-lipotropin, Nature, 260 (1976) 622-4.

Machelska, H., Mousa, S.A., Brack, A., Schopohl, J.K., Rittner, H.L., Schafer, M. and Stein, C., Opioid control of inflammatory pain regulated by intercellular adhesion molecule-1, J Neurosci, 22 (2002) 5588-96.

Machelska, H. and Stein, C., Leukocyte-derived opioid peptides and inhibition of pain, J Neuroimmune Pharmacol, 1 (2006) 90-7.

Malan, T.P., Jr., Ibrahim, M.M., Deng, H., Liu, Q., Mata, H.P., Vanderah, T., Porreca, F. and Makriyannis, A., CB2 cannabinoid receptor-mediated peripheral antinociception, Pain, 93 (2001) 239-45.

Massi, P., Vaccani, A. and Parolaro, D., Cannabinoids, immune system and cytokine network, Curr Pharm Des, 12 (2006) 3135-46.

Massotte, D. and Kieffer, B.L., A molecular basis for opiate action, Essays Biochem, 33 (1998) 65-77.

Mousa, S.A., Machelska, H., Schafer, M. and Stein, C., Immunohistochemical localization of endomorphin-1 and endomorphin-2 in immune cells and spinal cord in a model of inflammatory pain, J Neuroimmunol, 126 (2002) 5-15.

Mousa, S.A., Cheppudira, B.P., Shaqura, M., Fischer, O., Hofmann, J., Hellweg, R. and Schafer, M., Nerve growth factor governs the enhanced ability of opioids to suppress inflammatory pain, Brain, 130 (2007) 502-13.

Munro, S., Thomas, K.L. and Abu-Shaar, M., Molecular characterization of a peripheral receptor for cannabinoids, Nature, 365 (1993) 61-5.

Nackley, A.G., Zvonok, A.M., Makriyannis, A. and Hohmann, A.G., Activation of cannabinoid CB2 receptors suppresses C-fiber responses and windup in spinal wide dynamic range neurons in the absence and presence of inflammation, J Neurophysiol, 92 (2004) 3562-74.

Ninkovic, M., Hunt, S.P. and Gleave, J.R., Localization of opiate and histamine H1-receptors in the primate sensory ganglia and spinal cord, Brain Res, 241 (1982) 197-206.

Ossipov, M.H., Lai, J., King, T., Vanderah, T.W., Malan, T.P., Jr., Hruby, V.J. and Porreca, F., Antinociceptive and nociceptive actions of opioids, J Neurobiol, 61 (2004) 126-48.

Parenty, G., Appelbe, S. and Milligan, G., CXCR2 chemokine receptor antagonism enhances DOP opioid receptor function via allosteric regulation of the CXCR2-DOP receptor heterodimer, Biochem J, 412 (2008) 245-56.

Patwardhan, A.M., Berg, K.A., Akopain, A.N., Jeske, N.A., Gamper, N., Clarke, W.P. and Hargreaves, K.M., Bradykinin-induced functional competence and trafficking of the delta-opioid receptor in trigeminal nociceptors, J Neurosci, 25 (2005) 8825-32.

Pert, C.B. and Snyder, S.H., Opiate receptor: demonstration in nervous tissue, Science, 179 (1973) 1011-4.

Portoghese, P.S., A new concept on the mode of interaction of narcotic analgesics with receptors, J Med Chem, 8 (1965) 609-16.

Potenzieri, C., Harding-Rose, C. and Simone, D.A., The cannabinoid receptor agonist, WIN 55, 212-2, attenuates tumor-evoked hyperalgesia through peripheral mechanisms, Brain Res, 1215 (2008) 69-75.

Reeh, P.W., Sensory receptors in mammalian skin in an in vitro preparation, Neurosci Lett, 66 (1986) 141-6.

Reynolds, D.V., Surgery in the rat during electrical analgesia induced by focal brain stimulation, Science, 164 (1969) 444-5.

Rittner, H.L., Brack, A., Machelska, H., Mousa, S.A., Bauer, M., Schafer, M. and Stein, C., Opioid peptide-expressing leukocytes: identification, recruitment, and simultaneously increasing inhibition of inflammatory pain, Anesthesiology, 95 (2001) 500-8.

Rittner, H.L., Labuz, D., Schaefer, M., Mousa, S.A., Schulz, S., Schafer, M., Stein, C. and Brack, A., Pain control by CXCR2 ligands through Ca2+-regulated release of opioid peptides from polymorphonuclear cells, Faseb J, 20 (2006) 2627-9.

Rittner, H.L., Lux, C., Labuz, D., Mousa, S.A., Schafer, M., Stein, C. and Brack, A., Neurokinin-1 receptor antagonists inhibit the recruitment of opioid-containing leukocytes and impair peripheral antinociception, Anesthesiology, 107 (2007) 1009-17.

Ross, R.A., Coutts, A.A., McFarlane, S.M., Anavi-Goffer, S., Irving, A.J., Pertwee, R.G., MacEwan, D.J. and Scott, R.H., Actions of cannabinoid receptor ligands on rat cultured sensory neurones: implications for antinociception, Neuropharmacology, 40 (2001) 221-32.

Russell, N.J., Schaible, H.G. and Schmidt, R.F., Opiates inhibit the discharges of fine afferent units from inflamed knee joint of the cat, Neurosci Lett, 76 (1987) 107-12.

Saade, N.E., Farhat, O., Rahal, O., Safieh-Garabedian, B., Le Bars, D. and Jabbur, S.J., Ultra violet-induced localized inflammatory hyperalgesia in awake rats and the role of sensory and sympathetic innervation of the skin, Brain Behav Immun, 22 (2008) 245-56.

Schafer, M., Carter, L. and Stein, C., Interleukin 1 beta and corticotropin-releasing factor inhibit pain by releasing opioids from immune cells in inflamed tissue, Proc Natl Acad Sci U S A, 91 (1994) 4219-23.

Shaqura, M.A., Zollner, C., Mousa, S.A., Stein, C. and Schafer, M., Characterization of mu opioid receptor binding and G protein coupling in rat hypothalamus, spinal cord, and primary afferent neurons during inflammatory pain, J Pharmacol Exp Ther, 308 (2004) 712-8.

Simon, E.J., In search of the opiate receptor, Am J Med Sci, 266 (1973) 160-8.
Smith, E.M., Opioid peptides in immune cells, Adv Exp Med Biol, 521 (2003) 51-68.

Smith, H.S., Peripherally-acting opioids, Pain Physician, 11 (2008) S121-32.

Stander, S., Gunzer, M., Metze, D., Luger, T. and Steinhoff, M., Localization of mu-opioid receptor 1A on sensory nerve fibers in human skin, Regul Pept, 110 (2002) 75-83.

Stein, C., Millan, M.J., Shippenberg, T.S., Peter, K. and Herz, A., Peripheral opioid receptors mediating antinociception in inflammation. Evidence for involvement of mu, delta and kappa receptors, J Pharmacol Exp Ther, 248 (1989) 1269-75.

Stein, C., Gramsch, C., Hassan, A.H., Przewlocki, R., Parsons, C.G., Peter, K. and Herz, A., Local opioid receptors mediating antinociception in inflammation: endogenous ligands, Prog Clin Biol Res, 328 (1990) 425-7.

Stein, E.A., Hiller, J.M. and Simon, E.J., Effects of stress on opioid receptor binding in the rat central nervous system, Neuroscience, 51 (1992) 683-90.

Stein, C. and Yassouridis, A., Peripheral morphine analgesia, Pain, 71 (1997) 119-21.

Szolcsanyi, J., Selective responsiveness of polymodal nociceptors of the rabbit ear to capsaicin, bradykinin and ultra-violet irradiation, J Physiol, 388 (1987) 9-23.

Szolcsanyi, J., Anton, F., Reeh, P.W. and Handwerker, H.O., Selective excitation by capsaicin of mechano-heat sensitive nociceptors in rat skin, Brain Res, 446 (1988) 262-8.

Taddese, A., Nah, S.Y. and McCleskey, E.W., Selective opioid inhibition of small nociceptive neurons, Science, 270 (1995) 1366-9.

Terenius, L., Characteristics of the "receptor" for narcotic analgesics in synaptic plasma membrane fraction from rat brain, Acta Pharmacol Toxicol (Copenh), 33 (1973) 377-84.

Tominaga, M., Ogawa, H. and Takamori, K., Possible roles of epidermal opioid systems in pruritus of atopic dermatitis, J Invest Dermatol, 127 (2007) 2228-35.

Waddell, P.J. and Lawson, S.N., Electrophysiological properties of subpopulations of rat dorsal root ganglion neurons in vitro, Neuroscience, 36 (1990) 811-22.

Wenk, H.N. and Honda, C.N., Immunohistochemical localization of delta opioid receptors in peripheral tissues, J Comp Neurol, 408 (1999) 567-79.

Wenk, H.N. and Honda, C.N., Silver nitrate cauterization: characterization of a new model of corneal inflammation and hyperalgesia in rat, Pain, 105 (2003) 393-401.

Wenk, H.N., Brederson, J.D. and Honda, C.N., Morphine directly inhibits nociceptors in inflamed skin, J Neurophysiol, 95 (2006) 2083-97.

Werz, M.A. and Macdonald, R.L., Heterogeneous sensitivity of cultured dorsal root ganglion neurones to opioid peptides selective for mu- and delta-opiate receptors, Nature, 299 (1982) 730-3.

Willis, W.D., Jr., Dorsal root potentials and dorsal root reflexes: a double-edged sword, Exp Brain Res, 124 (1999) 395-421.

Young, W.S., 3rd, Wamsley, J.K., Zarbin, M.A. and Kuhar, M.J., Opioid receptors undergo axonal flow, Science, 210 (1980) 76-8.

Young, A.R., Guy, R.H. and Maibach, H.I., Laser Doppler velocimetry to quantify UV-B induced increase in human skin blood flow, Photochem Photobiol, 42 (1985) 385-90.

Zhou, L., Zhang, Q., Stein, C. and Schafer, M., Contribution of opioid receptors on primary afferent versus sympathetic neurons to peripheral opioid analgesia, J Pharmacol Exp Ther, 286 (1998) 1000-6.